Masters Program in Geospatial Technologies

PRECISION AGRICULTURE USING UNMANNED AERIAL SYSTEMS

Mapping Vigor's Spatial Variability on Low Density Agricultures using a Canopy Pixel Classification and Interpolation Model

Pedro Pais Penedos

Dissertation submitted in partial fulfilment of the requirements for the Degree of *Master of Science in Geospatial Technologies*

NOVA IMS Information Management School
UNIVERSITAT JAUME·I
Westfälische Wilhelms-Universität Münster

PRECISION AGRICULTURE USING UNMANNED AERIAL SYSTEMS

Mapping Vigor's Spatial Variability on Low Density Agricultures using a Canopy Pixel Classification and Interpolation Model

Dissertation supervised by

MSc Alexandre Santos

PhD Marco Painho

PhD Carlos Granell

February 2017

Masters Program in Geospatial Technologies

PRECISION AGRICULTURE USING UNMANNED AERIAL SYSTEMS

Mapping Vigor's Spatial Variability on Low Density Agricultures using a Canopy Pixel Classification and Interpolation Model

Pedro Pais Penedos

Dissertation submitted in partial fulfilment of the requirements for the Degree of *Master of Science in Geospatial Technologies*

NOVA IMS Information Management School
UNIVERSITAT JAUME·I
WESTFÄLISCHE WILHELMS-UNIVERSITÄT MÜNSTER

PRECISION AGRICULTURE USING UNMANNED AERIAL SYSTEMS

Mapping Vigor's Spatial Variability on Low Density Agricultures using a Canopy Pixel Classification and Interpolation Model

Dissertation supervised by

MSc Alexandre Santos

PhD Marco Painho

PhD Carlos Granell

February 2017

ACKNOWLEDGMENTS

To PhD Carlos Granell.

To PhD Chaplin Williams.

To Eduardo Penedos.

To MSc João Ferreira.

To PhD Lisa Fischell.

To Mafalda.

To Maria.

To PhD Marco Painho.

To Mosto.

To PhD Sara Ribeiro.

To PhD Ana Costa.

PRECISION AGRICULTURE USING UNMANNED AERIAL SYSTEMS

Mapping Vigor's Spatial Variability on Low Density Agricultures using a Canopy Pixel Classification and Interpolation Model

ABSTRACT

It is becoming more present in agriculture's practices the use of Unmanned Aerial Systems with sensors capable of capturing light, in the visible and in longer wavelengths of the electromagnetic spectrum once reflected on the field. These sensors have been used to perform Remote Sensing also in other knowledge fields, describing phenomenon without the risk, cost and the time consuming processes associated with in site samples collection and analysis by a technician or satellite imagery acquisition. The Vegetation Indexes developed can explain the vigor of the cultivation and its data collection processes are more cost and time efficient, allowing farmers to monitor plant grow in every critical stage. These Vegetation Indexes started by being calculated from satellite and airborne imagery, one of the main source for crop management tools, however UAS is becoming more present in Precision Agriculture, achieving better spatial and temporal resolution. This gap in spatial resolution when studying low density cultivations like olive groves and vineyards, creates Vegetation Index's maps polluted with noise caused by the soil and therefore difficult to interpret and analyse. Hence, when the agriculture has spaced and low density vegetation becomes challenging to understand and extract information from these vegetation index's maps regarding different spatial variability patterns of the tree canopy vigor. In these cases, where vegetation is spaced it is important to filter this noise. A Classification Model was developed with the objective of extracting just the vegetation's canopy data. The soil was filtered and the canopy data interpolated using spatial

analysis tools. The final interpolated maps produced can provide meaningful information regarding the spatial variability and be used to support decision making, identifying critical areas to be intervened and managed, or be used as an input for Variable Rate Technology applications.

PRECISION AGRICULTURE USING UNMANNED AERIAL SYSTEMS

Mapping Vigor's Spatial Variability on Low Density Agricultures using a Canopy Pixel Classification and Interpolation Model

ABSTRACT (Português)

O uso de Sistemas Aéreos Não Tripulados ou drones é cada vez mais frequente nas práticas agrícolas, com sensores que captam luz em diferentes comprimentos de onda depois de refletidos na área de estudo. Estes sistemas são utilizados para levantamento de dados remotamente em outros campos de estudo, devido à sua versatilidade. Sem os riscos, custos associados quando comparados com os processos complexos e longos de recolha e análise de amostras por técnicos ou aquisição de imagens de satélite de alta resolução. Estes sensores e os Índices de Vegetação a partir deles desenvolvidos conseguem ajudar a explicar o vigor da vegetação e os processos de coleta de dados com estes sistemas aéreos são mais eficientes em termos de custo e tempo, permitindo que os agricultores monitorizem as culturas e em todas as etapas críticas. Estes Índices de Vegetação começaram a ser calculados com recurso a imagens de satélite e aéreas como fonte principal para gestão de explorações agrícolas, mas agora também os sistemas aéreos não tripulados são usados para os mesmos fins conseguindo resultados com melhor resolução, tanto espacial como temporal. Esse aumento na resolução espacial, nos casos de agriculturas de baixa densidade como o olival e a vinha cria mapas difíceis de interpretar devido ao ruido causado pelo solo e outros objectos. Quando as culturas têm uma distribuição espaçada e de baixa densidade com solo visível, pode ser difícil compreender e extrair conhecimento destes mapas em relação a diferentes áreas onde os níveis críticos se concentram. Nestes casos, é importante filtrar o solo, permitindo

assim a interpretação dos mapas de Índices Vegetativos e a extração de informação útil para a agricultura que de outra maneira seria difícil e demoroso. Um modelo de classificação foi desenvolvido com o objetivo de extrair apenas os pixéis das copas das árvores. A vegetação em estudo será filtrada e em seguida os valores de NDVI dos pixéis das copas interpolados usando ferramentas de análise espacial. Estes mapas finais apresentam informações uteis em relação aos padrões de variabilidade espacial do vigor das agriculturas e podem ser utilizados como ferramenta de apoio à tomada de decisão, identificando e segmentando áreas prioritárias a serem investigadas, ou podem ser usadas como input em sistemas VRT.

KEYWORDS

Geographical Information Systems

Geospatial Data Mining

Geostatistics

Green Normalized Difference Vegetation Index

Image Classification

ISO Cluster Analysis

Kriging Interpolation

Multispectral Sensors

Normalized Difference Red Edge Index

Normalized Difference Vegetation Index

Precision Agriculture

Remote Sensing

RGB Imagery

Spatial Autocorrelation

Spatial Variability

Unmanned Aerial Systems

Variable Rate Technology

Vegetation Vigor

KEYWORDS (Português)

Agricultura de Precisão

Análise de Cluster ISO

Autocorrelação Espacial

Classificação de Imagem

Data Mining Geoespacial

Geoestatística

GNDVI

Imagens RGB

Índice de Vegetação

Interpolação Kriging

NDRE

NDVI

Sensores Multiespectrais

Remote sensing

Sistemas Aéreos Não Tripulados

Sistemas de Informação Geográfica

Variabilidade Espacial

Variable Rate Tecnology

Vigor da Vegetação

ACRONYMS

DEM – Digital Elevation Model

DOC – Denominação de Origem Controlada

DSM – Digital Surface Model

DTM – Digital Terrain Model

GIS – Geographic Information Systems

GNDVI – Green Normalized Difference Vegetation Index

GPS – Global Position System

NDRE – Normalized Difference Red Edge Index

NDVI – Normalized Difference Vegetation Index

UAS – Unmanned Aerial Systems

UAV – Unmanned Aerial Vehicle / Drone

VRT – Variable Rate Technology

INDEX OF THE TEXT

Pag.

ACKNOWLEDGMENTS i
ABSTRACT ii
ABSTRACT (Português) iv
KEYWORDS vi
KEYWORDS (Português) vii
INDEX OF THE TEXT ix
INDEX OF TABLES xi
INDEX OF FIGURES xii
1 INTRODUCTION 1
2 LITERATURE REVIEW 2
3 METHODOLOGY 7
3.1 Study Area 8
3.1.1 Vineyard 10
3.1.2 Olive grove 11
3.2 UAV Imagery Collection and Processing 11
3.3 Data Pre-Processing 12
3.4 Classification Model 13
3.4.1 Vine Classification 15
3.4.2 Olive Tree Classification 15
3.5 Inverse Distance Weighted Interpolation 16
3.6 Kriging Interpolation 16
4 RESULTS 17
4.1 UAV Imagery Collection and Processing 17
4.2 Vine Classification 18
4.2.1 Principal Components Analysis 18
4.2.2 Outlier and Cluster Analysis 20
4.3 Olive tree Classification 22
4.3.1 Principal Components Analysis and ISO Cluster Analysis 22
4.3.2 Outlier and Cluster Analysis 24

4.4 Exploratory Spatial Point Data Analysis 26
4.5 Inverse Distance Weighted Interpolation 30
4.6 Kriging Interpolation 36
5 DISCUSSION 44
6 CONCLUSIONS 46
BIBLIOGRAPHIC REFERENCES 47

INDEX OF TABLES

Table 1. Dissertation's Chronogram. 2
Table 2. Quality check report. 17
Table 3. Correlation Matrix vineyard PC Analisys. 18
Table 4. Principal Components vineyard classification. 18
Table 5. Correlation Matrix olive tree PC Analisys. 22
Table 6. Principal Components olive grove classification. 22
Table 7. Searching neighbourhood table. 30

INDEX OF FIGURES

Figure 1. An example of the resolution between different systems. 3
Figure 2. Dissertation Workflow. 8
Figure 3. Herdade do Esporão – Study Area. 9
Figure 4. Vineyard's RGB Imagery. 10
Figure 5. Vineyard's DTM Raster. 10
Figure 6. Olive grove's RGB Imagery. 11
Figure 7. Olive grove's DTM Raster. 11
Figure 8. Classification Model. 13
Figure 9. Classified polygons and cleanning selection for the vineyard. 19
Figure 10. Vineyard's Spatial Autocorrelation by distance graph. 20
Figure 11. Ansellin's local Moran's I map for the vineyard. 21
Figure 12. Classified polygons and cleanning selection for the olive grove. 23
Figure 13. Olive grove's Spatial Autocorrelation by distance graph. 24
Figure 14. Ansellin's local Moran's I map for the olive grove. 25
Figure 15. Point data posting. 26
Figure 16. Lower Mean NDVI selection. 27
Figure 17. Point data posting. 28
Figure 18. Lower Mean NDVI selection. 29
Figure 19. Vineyard predicted surface 31
Figure 20. Vineyard contour lines map. 32
Figure 21. Olive grove predicted surface. 33
Figure 22. Olive grove contour lines map. 34
Figure 23. Mean and standard deviation maps of the mean NDVI data for the vineyard. 35
Figure 24. Mean and standard deviation maps of the mean NDVI data for the olivegrove. 36
Figure 25. Kriging searching neighbourhood table and semivariogram. 37
Figure 26. Predicted surface map. 38
Figure 27. Prediction standard error map. 39
Figure 28. Predicted surface map. 40
Figure 29. Prediction standard error map. 41

Figure 30. The original NDVI map for the vineyard. 42
Figure 31. The original NDVI map for the olive grove. 42
Figure 32. Final Vigor's Variability Map for the vineyard. 43
Figure 33. Final Vigor's Variability Map for the olive grove. 44

1 INTRODUCTION

The introduction of new disciplines and technologies to agriculture such as GIS, Geo-statistics, Remote Sensing, Geospatial Data Mining, GPS, VRT and now UAS opened up new applications possibilities for farming, increasing competitiveness in the sector by improving quality, yield and both economic and environmental sustainability. UAS allow the user to perform Remote Sensing, using sensors to quantify the reflection of different wavelengths by an object. Although RS has been strongly associated with satellite or aircraft imagery it can be also collected using other devices and technologies, like UAS. Using a sensor attached to a UAV, is possible to fly over the cultivation creating a structured record of images in known coordinates. These pictures can be processed in software's that produces a series of different outputs, like Point Clouds, Orthophotos, DEM's, and also Vegetation Indexes maps if a Multispectral camera is used. UAS can produce better resolution imagery bringing new challenges for image processing but also new opportunities and possibilities to improve variability mapping technics. From these sensors is possible to calculate Vegetation Indexes thus quantifying and qualifying the variability in a given plot (Ortega & Esser, 2002). There are several Vegetation Indices, each allow the spatial variability analysis of quality and productivity, creating new management areas for the application of fertilizers or water, reducing production costs as well as environmental impacts. Low density agriculture present additional challenges to understand and extract knowledge from the vegetation index's maps regarding different spatial variability patterns of the vegetation's vigor, due to the noise caused by the soil. In this dissertation, Multispectral and RGB imagery was collected from the study areas, a classification model was developed with the objective of extracting only the pixels from the agriculture's canopies. The vegetation under study was filtered and then the vegetation's Normalized Difference Vegetation Index values interpolated using spatial analysis tools with the objective of covering the soil areas with data from neighbouring canopies' values. These interpolated final maps reveal useful information that can be used as a spatial variability visualization tool to support decision making, identifying and differentiating

critical areas to be investigated and managed. These maps can also be easily adapted and used in VRT applications minimizing costs in fertilization and water and reducing environmental impact. In Table 1. is possible to see the dissertation's chronogram.

Dissertation's Chronogram

Tasks	Aug.	Sept.	Oct.	Nov.	Dez.	Jan.
Exploring Topic and Related work	Literature Review	- Intro - Methodologies	Techniques	Spatial Analysis	Literature Review	Conclusions
Access to / Collecting Data	Collecting Data	Collecting Data	Olive Trees and Vines: -Multispec imag. -RGB Imagery			
Preprocessing Data	Vine Trees -Multispec imag.	Image processing Creating Ortho's/ DEM's/	Creating Ortho's/ DEM's/ Consolidating data			
Exploratory Data Analysis		Exploration of Precision Agriculture Methodologies and technics	Calculation of indexes CP/F Analysis STD Var			
Segmentation/ Classification			ISO Cluster Analysis Cluster and Outlier analysis	Cluster and Outlier analysis Cleaning and smoothing Selection		
Spatial Analysis				- Sampling - Interpolation IDW	Interpolation Kriging	
Writing / Submission	Proposal	Literature Review	- Intro - Methodologies	Preprocessing - Methodologies	Spatial Analysis	Conclusions

Table 1. Dissertation's Chronogram.

2 LITERATURE REVIEW

Precision Agriculture consists in measuring, analysing and developing plans to manage the variability present in crops. Different management areas can be created corresponding to their characteristics with the goal of increasing efficiency while preserving resources. Two types of variability can happen, spatial variability is associated with intrinsic causes, such as, topography, soil characteristics, plant vigor, microclimate and cultural techniques. In this case, the farmer has a smaller intervention capacity, but nevertheless, there are decisions and interventions that can influence the performance and spatial variability of an agriculture like the origin of the vegetal material, paring, clone selection, or irrigation. Temporal variability in other hand is associated with changes in cultural techniques, weather conditions and attacks of pests, fires

that may give rise to annual losses (Proffit et al., 2006). Agriculture production is affected by multiple factors which can cause variations in yield and in the quality of the harvest (Ribéreau-Gayon, 2006). There are many instruments and technologies used to control and monitor this variability throughout the whole growing phase, some of them require the data to be collected using time consuming ground sampling technics, as well as, costly instruments and materials. RS can be used to measure and map this spatial variability using sensors that capture light's reflection on the terrain. RS is heavily associated with satellite imagery analysis but UAS's are now being used to collect imagery in specific electromagnetic wavelengths more efficiently. UAS allows for temporal resolution to be maximized to whenever the imagery is needed, and with better spatial resolution. This data can be later processed allowing the both variabilities to be analysed using GIS.

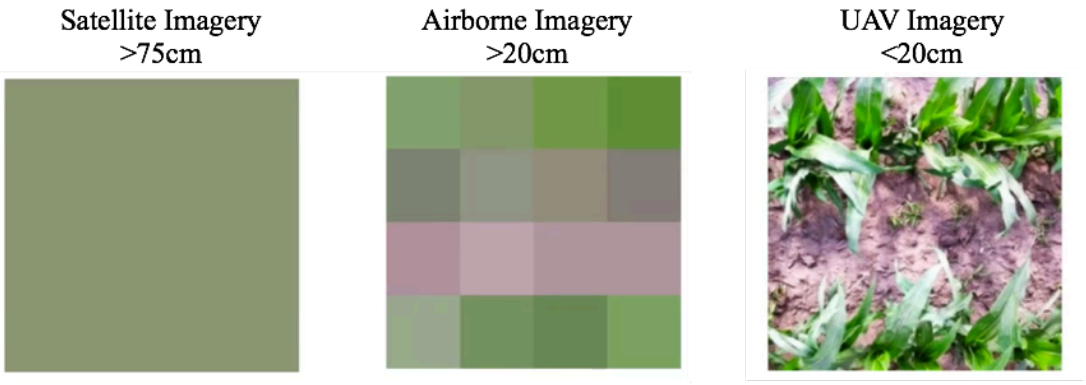

Figure 1. An example of the resolution between different systems.

The gap in spatial resolution shown in (Figure 1.) between the different sensor systems is clear and opens up new possibilities for application development in the Precision Agriculture field. Satellite and airborne imagery has been used globally in agriculture and while in dense agricultures like cereals it's application can bring value to the farmer, the same is not so linear when low density agricultures are being studied like vineyards and olive groves, due to the presence of soil and other vegetation (Matese et al., 2015). In these cases, low spatial resolution images represent an average of the vegetation canopy and soil, thus not representing the intra-canopy spatial variability. It is possible to assume that when a higher amount of soil is present, low resolution imagery produces a biased representation of the intra-vineyard spatial variability. In

order to fully exploit this resolution gap created by UAS, is required to understand the intervening variables that cause this variability so that the crops have a better consistency in the long run, qualitatively and quantitatively. Precision Agriculture was designed to monitor and manage the spatial variability of physical, chemical and biological variables that are intertwined with the productivity of an agriculture. By investing in precision agriculture technologies and knowledge, production efficiency and quality can be maximized, while minimizing risk and the activity's environmental impact (Pires, 2008). The main goal is to control the vigor's spatial variability by identifying areas with distinct value's concentration patterns in the agriculture and providing the tools to manage these areas separately. For this purpose, a wide range of tools and technologies are used, enabling farmers to make a more robust and oriented decision making (Proffit et al., 2006). Precision Agriculture objectives involves the identification and segmentation of areas with different and similar growth characteristics. Consists in finding spatial or temporal patterns for different behaviours using the data collected in the field, improving efficiency and production by using segmented management zones for irrigation and fertilization, as an example. Implementation of Precision Agriculture technics allows for knowledge based decision making to occur, improving production efficiency, profitability and sustainability. Examples of currently used applications varies from yield mapping, terrain modelling, water management and drainage systems. It is possible also the calculation of indexes related to vegetation vigor, and from them create prescription maps, for water irrigation or nitrogen applications. Prescription maps can help optimizing resources, they can be loaded to a Variable Rate Technology System, a system that allows for a variable amount to be delivered to a determined location in the farm, using GPS. Vegetation's Indexes maps can be analysed with the objective of monitor vegetation vigor or used for high and continuous water stress (Baluja et al., 2012), pathogen detection (Zarco-Tejada et al., 2012), estimation of nitrogen level (Tokekar et al., 2013), mapping invasive weeds and monitor herbicide applications (Xiang et al., 2011). According to Proffit et al., in 2006 and referring to vines in specific, creates a Precision Agriculture structure based on a cyclic process consisting on 3 phases: Phase I: Monitoring the behaviour of the crops

and collecting data using technologies such as remote sensing, soil sampling data with geology information, nutrients concentration and fruit quality data that will be essential for solving the problem by analysing the results. Phase II: Interpretation and evaluation of the data collected, using spatial analysis software's. Phase III: Implementation plans and crop management technics which will differentiate the treatments by areas and time such as irrigation, fertilization, phytosanitary treatments, yield, cultural operations, etc. Vegetation indexes have an important role in PA by describing and mapping the vigor of the agriculture being analysed. With Multispectral cameras is possible to calculate Vegetation Indexes, they allow the study of the vegetation vigor's spatial variability and the data collection processes with these aerial systems are more cost-efficient and time-efficient, allowing farmers to monitor growth in large areas and in every critical stage. These cameras capture different wavelength intervals, like for example the RGB colors, however, other intervals can be useful to study vegetation like the infrared or the red edge. These Vegetation Indexes have been calculated using mainly satellite and aerial imagery and now UAV's are raising the bar in terms of resolution. This difference in spatial resolution between different systems in the case of low density crops such as olive groves and high resolution imagery creates Vegetation Index maps difficult to interpret due to soil related noise. When farms have sparse and low-density vegetation, it can be difficult to understand and extract information from these maps in relation to different areas where critical levels are concentrated. In cases where vegetation is spaced and soil is present between the crops, it is important to create new technics and methodologies capable of filtering the canopies, allowing the understanding of the spatial variability without the noised caused by the soil and other vegetation (Salamí et al, 2014). There are different indexes that have been developed using Multispectral Sensors and with multiple applications in agriculture: The Normalized Difference Vegetation Index calculated using the following equation, (NIR - RED) / (NIR + RED) (Rouse et al., 1974). The NDVI is one of the more commercially used indexes by farmers, it is used for mapping vigor, differences in water availability, nutrient content of the leaf and also used to estimate yield. For the same purpose there are others indexes, like Green

NDVI, calculated using the following equation, (NIR - GREEN) / (NIR + GREEN) (Gitelson et al, 1996). This Index was found to have a linear relationship with Chlorophyll and to be much more sensitive to different concentrations of the substance. The Normalized Difference Red Edge is also used for mapping vigor, stress detection, Nitrogen uptake monitoring and can only be calculated using the Near-Infrared band and the Red Edge band. NDRE is useful for mapping the fertilizer demand variability and is sensitive to leaf density, better describing the vigor in cases where the NDVI shows saturated values due to high vigor leaf concentration. The use of Digital Elevation models makes possible the handling of the data concerning the altimetry of both the terrain plus the features in the study area. Normally used in a raster format, it gives information about the altimetry characteristics and can be used in different scales. In this Dissertation is critical to identify the differences between two types of DEM's: The Digital Surface Model, a Digital Model of the surface of the study area, in this is included features like trees or building, plus the terrain level. And the Digital Terrain Model, a Digital Model of the terrain, this excludes features present above the ground level, showing just the terrain of the area. Different methodologies can be used for the classification model like a point cloud, a pixel based or an object based classification. A pixel based classification although working with pixels, enables the introduction of multiple variables in the model, while other classifications typically do not allow this selection of input variables. Spatial autocorrelation is based on the degree of similarity between one location and neighbour locations. It measures the degree to which the occurrence of an event in one area makes more or less probable, the occurrence of a similar event in a neighbouring area. It quantifies spatial dependence or correlation of a variable with itself. Interpolation is a estimation procedure that calculates values at non-sampled locations taking in consideration sampled locations as input data source. It is a mathematical model that allow performing attribute predictions at any location of a surface. There are interpolators which the estimated value for each sampled location is equal to the observed sample, these are called exact interpolators, in these cases the predicted surface passes through the sampled data values. Interpolation can also be used for analysing spatial continuity, evaluating the

main spatial patterns of the physical phenomenon like proportional effect, anisotropic pattern or global trends. Proportional effect is present when a relationship between local means and local standard-deviations is found. Isotropic patterns are found when the spatial autocorrelation structure is independent of direction, or the same in all directions. The Inverse Distance Weighting interpolator, uses the sampled values surrounding the prediction locations to predict a value for every non sampled location, based on the supposition that things that are close by share more similar behaviours than those that are farther apart. Kriging, an exact interpolator, is a geostatistical procedure that generates an estimated surface from a scattered set of points with observed z-values of a continuous attribute. It creates variograms and covariance functions to estimate the statistical dependence or spatial autocorrelation and predicts the unknown values in a surface.

3 METHODOLOGY

The methodology followed a workflow shown in Figure 2., the gathering of the data and image processing stages were crucial steps for the accomplishment of the objectives in this dissertation. Since both data was collected and consolidated from the Multispectral and RGB sensors, both in different flights and UAV's, it was required the geo-referencing of different Multispectral bands in relation to one to be executed. Pix4Dmapper Pro was used as an image processing tool, converting the data from the sensors to different formats, like point clouds, Orthophotos and raster's. After creating all the bands, consolidating the data by geo-referencing, clipping the images to the study area, calculating the indexes and final variables, was possible to begin the classification model development in ArcGIS. The methodology was developed initially using the vineyard and later adapted to the olive grove. Enough discriminatory characteristics had to be inserted in to the classification model in order to classify the target features, thus multiple variables were inserted in the Classification model using the Principal Components tool in ArcGIS. The first three tasks were important for the final results' potential, but it is of same importance the classification and the Exploratory Data Analysis in order to

assure a consistent sampling method for the interpolation model development phase. After the Classification Model developed and the features segmented, sampling of the canopies was done by creating points in each polygon.

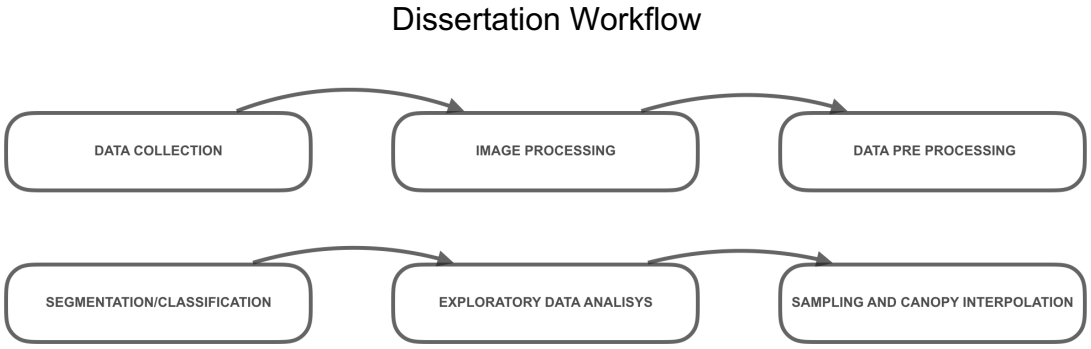

Figure 2. Dissertation Workflow.

NDVI statistics were extracted by polygon and an Interpolation model was developed in order to map the vigor's spatial variability of the canopies. This Interpolation allows the visual interpretation of the vigor's spatial variability in the segmented vegetation and can reveal areas where there is vegetation with lower or higher NDVI values without the noise caused by the soil NDVI values, close to zero.

3.1 Study Area

The study area selected is inserted in Reguengos de Monsaraz, an area characterized by many cork oak forests, located near Évora, Portugal. (Figure 3.) In the centre of the Alentejo Region, Herdade do Esporão is a farm covering 691,9 hectares of vineyard, olive groves and others organic cultures. The average temperature recorded in the region is between 15 and 17 Cº (59/63 Fº), showing high thermal amplitudes, with a yearly rainfall of 550ml/m2 and an average of 313 sunny days during the entire year. (Esporão, 2017) Several technics are used to improve biological practices of natural resources in Herdade do Esporão. Composting is done from by-products produced in the farm, green manure and green pruning are technics used to minimize fertilizers' requirements, just like the planting of Hedgerows as auxiliary fauna and the construction of shelters for bats in order to prevent pets and consequently

chemical treatments. Likewise, livestock is used in the vineyard during the winter, this helps controlling the weed growing. Water irrigation in Esporão is made with a drip irrigation system.

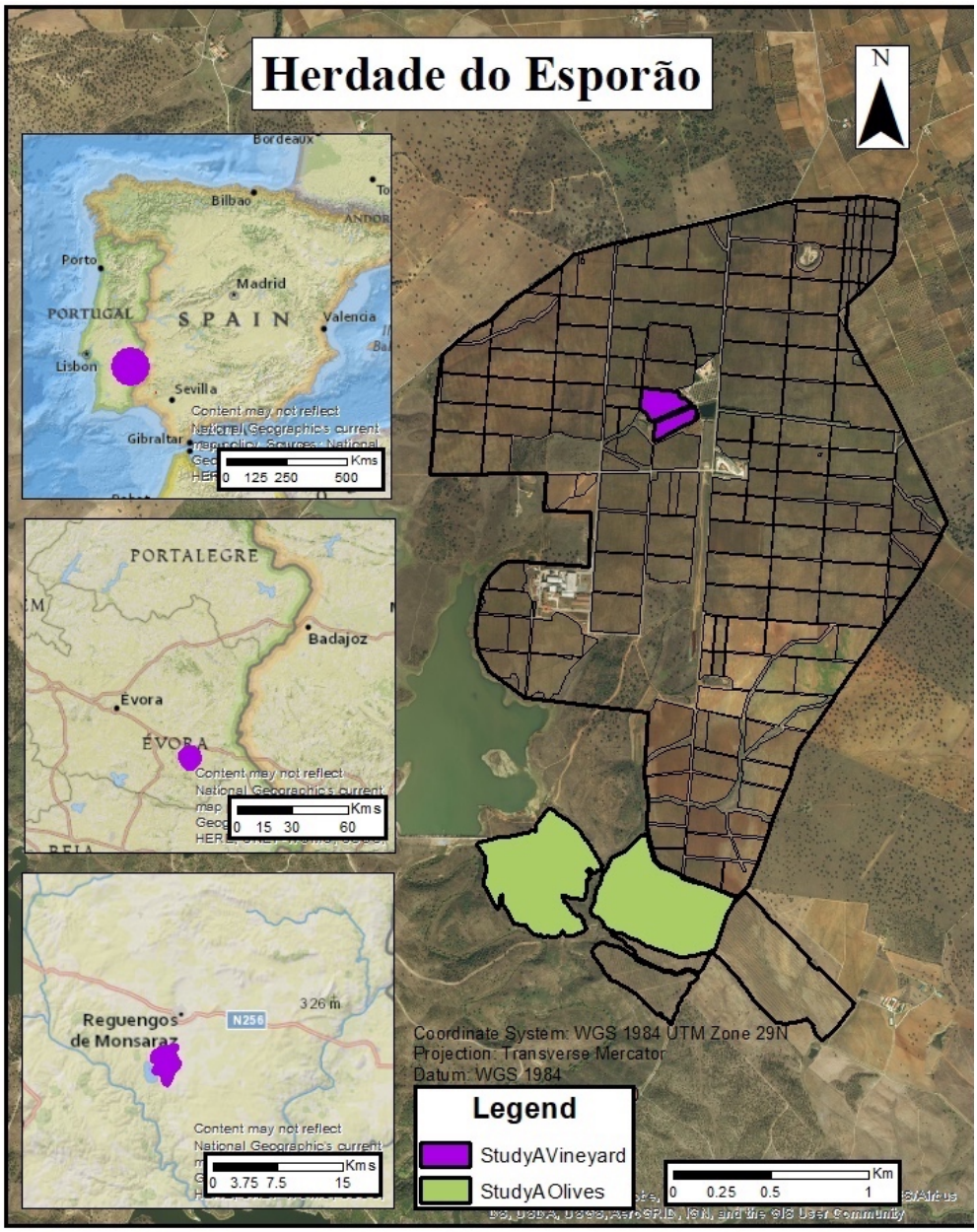

Figure 3. Herdade do Esporão – Study Area.

These biological practices and management plans are implemented with the main goal of eliminating the use of synthetic materials in the soil. In this dissertation two different agricultures were selected, the vineyard and the olive grove (Figure 3.), both agricultures have a considerable percentage of visible soil, therefore suitable agricultures for the objectives proposed in this

dissertation. The terrain elevation in the vineyard study area is in its majority plain, especially the area selected. In the olive grove is possible to see bigger slopes that can affect the drainage of water and subsequently the vegetation vigor.

3.1.1Vineyard

The area selected was chosen taking in consideration mainly the species variety. 40 different grape varieties are grown in Esporão, therefore it is expected that different species have distinct growing dynamics as well as different vigor levels in the same instant. So in order to map this vigor's spatial variability, one area containing just one variety of vine was selected. The altimetry data of the Digital Terrain Model showed that the area selected is overall plain and does not have any steep slopes or drainage systems as shown in Figure 5.

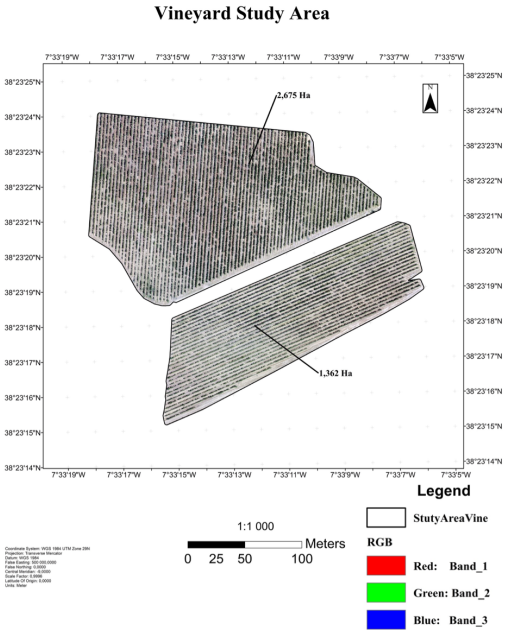

Figure 4. Vineyard's RGB Imagery.

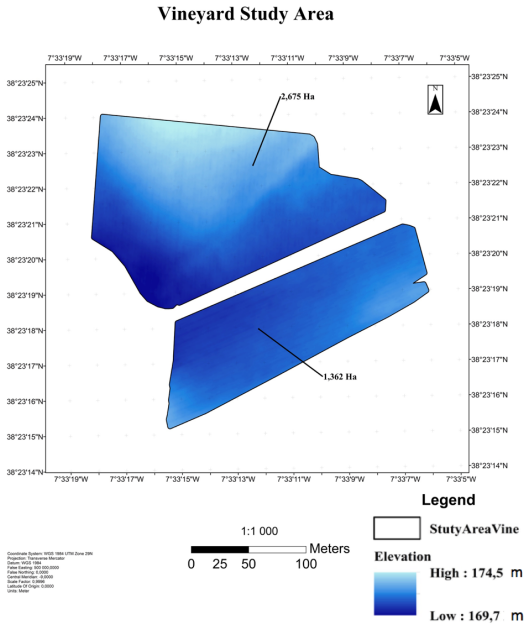

Figure 5. Vineyard's DTM Raster.

The vine variety present in the study area is named Tempranillo or also called Aragonez, it is widely used in the Mediterranean for winemaking as well as used in certain Porto wines. The vineyard study area has 4,362 ha as shown in Figure 4.

3.1.2Olive grove

Esporão has 4 different varieties of Olives growing in the property and more than 50 ha belong to the Cobrançosa variety. For the olive grove study area, two olive groves were selected, each one has around 26 ha, as it is shown in Figure 6 and 7, where also the RGB imagery and the DTM are presented. In the olive grove case, information about the presence of more than one olive tree species in the study area was not available. In this study area, elevation can be a contributing factor for vigor's spatial variability, since it covers a larger size. The presence of a manmade water drainage system can be a sign of accumulation of water in along some parts of the olive grove, as it is possible to see in Figure 6 and 7. At the site was possible to see that olive trees on both olive groves had different physiognomy, thus it is suspected that they have distinct ages and consequently different growing dynamics.

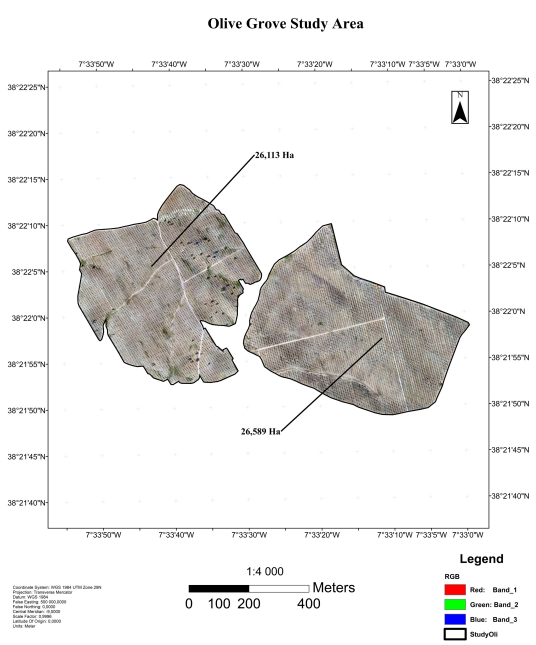

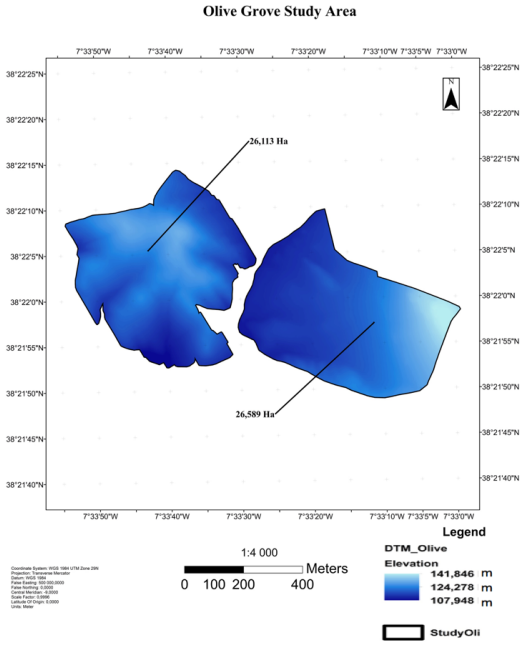

Figure 6. Olive grove's RGB Imagery. Figure 7. Olive grove's DTM Raster.

3.2 UAV Imagery Collection and Processing

The image acquisition date for the olive grove study area is September 2017 and August 2017 for the Vineyard. This farm is located in the Alentejo region where the weather is normally dry with temperatures reaching 40º C or 104º F, in the summer. In order to collect the images from the study area, two different

UAV's were used, one to collect the RGB imagery, and another dedicated to the Multispectral imagery. RGB imagery was acquired using a DJI Phantom Pro and the respective UAV stock camera with 20 Megapixels. For the Multispectral images, a e-Bee was used, a fixed-wing UAV from Sensefly with a 16 Megapixels Parrot Sequoia Multispectral Camera attached. The wind speed checked in the planning stage in a wind forecast website and confirmed at the spot, was below 10 knots, with a Northern direction. All missions were planned at an altitude of 120 meters, guaranteeing that the spatial resolution achieved was less than 3 cm for the RGB imagery and less than 20 cm for the Multispectral imagery. The software's used for the flight planning were distinct for each UAV, for the e-Bee the Sensefly commercial software was used, while the RGB imagery collection flight was planned using Pix4D Capture. Radiation calibration was executed prior to each flight with the Sequoia sensor allowing a better post image analysis. After the image collection phase, imagery collected was consolidated and processed separately using Pix4d mapper Pro 3.1.23, creating the point clouds that are later processed in to DEM's and the different bands from the RGB and Multispectral sensor. Corresponding to the location of the study areas, the Projected Coordinate System used to process the images in Pix4d Mapper Pro was WGS 1984 UTM 29N as it is shown in every map in this dissertation.

3.3 Data Pre-Processing

The Data Pre-Processing phase started by geo-referencing the Multispectral bands in relation to the R.G.B. images, using a minimum of 6 manual tie points and 2nd order polynomial transformations. After clipping all the geo-referenced layers to the study area's polygons, this includes the RGB, the DEM's (DTM/DSM) and the Multispectral bands. NDVI, GNDVI and NDRE indexes were calculated from the respective Multispectral bands just like the difference between the DSM and DTM, producing a map filtering just the features above ground level and its elevation data. An important aspect to take in consideration is that the Vegetation Indexes were calculated using the bands from the Multispectral sensor and not the red or green band from the RGB sensor. In addition to that, before the classification stage, all bands were standardized to

the same interval (0-225), assuring the classification model, depending on the variance present in the data distribution, gives the same explanatory power to all variables independently of the different variable's range. This was done in the Raster Calculator Tool with the following formula:

$$StdR = ((R - MinR) * (MaxS - MinS) / (MaxR - MinR)) + MinS,$$

Where,
StdR is the Standardized Raster,
R is the original Raster,
MaxR and MinR are the max and the min value of R,
MaxS and MinS are the max and the min value of interval to give to StdR.

3.4 Classification Model

In the classification stage the same general methodology was used in both study areas. (Figure 8.) Any distinction between the two methodologies and details are going to be clarified during 3.4.1. and 3.4.2. This can be explained by the different physiognomy characteristics in the study areas like the size, geometry, shape, vegetation density.

Classification Model

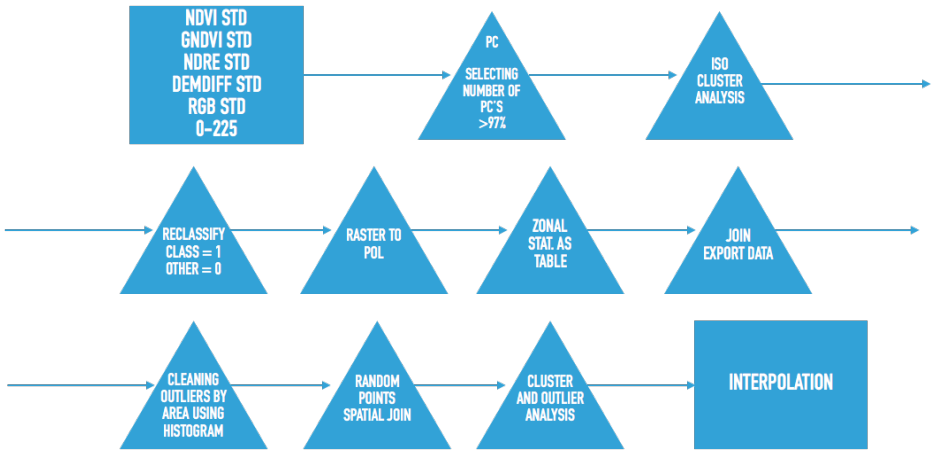

Figure 8. Classification Model.

For example, in the olive grove there are old Cork Oak trees spread through the field just like there is a constructed water drainage system covered with a white sandstone that reflects light more than the ground around it. With all the variables standardized the Principal Components analysis was performed selecting enough PC's in order to explain at least 97% of the variance present in the data. The first Principal Components analysis was executed with the

exploratory purpose of selecting the number of Principal Components to be used in the second analysis. A second Principal Components Analysis was performed selecting this time just the number of Principal Components resulting from the first analysis made, this result was used as an input for the ISO Cluster Classification tool. The output resolution selected was the same as the largest cell size in all input raster's (20 cm), thus avoiding the use of resampling techniques. The ISO Cluster Classification tool was used to categorize the image depending on different trends in Principal Components values. This tool was used to perform a sequence of unsupervised classifications on the different Principal Components selected and allowed the segmentation of the vines and olive trees using the Reclassify tool with a binary classification. Cells representing the vines or olive trees were classified with the value 1, while the soil and other vegetation was classified with the value 0. After converting the reclassified raster to polygons, representing the vines and olive trees, statistics about the NDVI were calculated and consolidated in relation with each polygon using the Zonal Statistics as Table, Join and Export Data. With the polygons created, the distribution by area was analysed and it was possible to conclude that a group of polygons had very small areas and they were not representing vines nor olive trees just like they were causing processing problems. Using the Histogram with the polygon's area distribution, polygons with areas smaller than the minimum expected and that showed a high frequency were excluded from the classification. After cleaning the group of polygons with small areas, less than 0,1479 m2 for the vineyard and less than 0,0398 m2 for the olive grove, zonal NDVI statistics as a table were calculated and joined in to the respective polygon data. Random points were generated inside the polygons with minimum distance between each and spatially joined to the respective polygon mean NDVI values. The statistic analysed was the mean NDVI variable, calculated by doing an average of the Sum of NDVI values per polygon, however other Vegetation Indexes can be used in this stage, like GNDVI or NDRE. Using the Random Points and Spatial Join tools, points were created inside the polygons, recording the respective polygon statistic. With the NDVI point data representing the vegetation, the spatial autocorrelation by distance was measured with the Incremental Spatial Autocorrelation tool and

subsequently a Cluster and Outlier Analysis was performed using the Anselin's Local Moran's I and the Moran's I tools. The Spatial Autocorrelation (Global Moran's I) tool was used to calculate the Moran's I statistic value, a z-score and a p-value that assess the significance related to the statistic. Given a set of points and an associated mean NDVI, the tool was used to evaluate whether the pattern existent is clustered as well as the presence of outliers. The outliers identified by the tool were subsequently not considered for the interpolation phase.

3.4.1Vine Classification

It is important to notice that in the vineyard study area, the NDRE band was showing a saturated surface caused by the NDRE band being corrupted, so in this case it was not included in the vine classification model. In the vineyard study area, it is difficult even with high spatial resolution to visually identify each vine's boundary since vines are usually intertwined, therefore each polygon created does not represent just one vine but a segment or a vector of vines. Due to this physiognomy of the vineyard, more than one point was placed in each polygon, since each polygon is representing a vector of vines. Random points were generated inside the polygons with 1 meter of minimum distance between each and spatially joined to the respective polygon mean NDVI values. The same was tested but using the NDVI raster to extract the raster values directly to the points and the results showed to be comparable to the method here proposed. This was done just to confirm if the mean NDVI per polygon calculation was attenuating the variability, however the same spatial patterns were identified.

3.4.2Olive Tree Classification

In the olive grove case, random points were generated inside the polygons with a 10 meters' minimum distance between each and spatially joined to the polygon mean NDVI values. In the olive grove case it was pretended that each polygon had just one point representing them, since in the classification phase was possible to discriminate single olive trees and their respective boundaries. The classification model was also capable to distinguish between oak trees and olive trees due to the use of multiple discriminatory variables like altimetry

related data. With this discriminatory power was possible to estimate the number of olive trees present in the olive grove study area.

3.5 Inverse Distance Weighted Interpolation

The Inverse Distance Weighting interpolator was used as an exploratory tool to investigate the presence of anisotropic patterns or global trends in the data. A neighbourhood tool of the Spatial Analyst toolbox was also used to compute the moving window statistics, with the objective of investigating the possibility of the existence of a proportional effect in the mean NDVI data. Multiple parameters were tested with the objective of reducing the associated errors. Results achieved are shown in Table 7., chapter 4.5. In the vineyard IDW's the power parameter selected was 2 with a 4 sector neighbourhood type. The maximum and minimum neighbours chosen were the ones that optimized the respective model, 3 and 8. A four sector type was selected with a major and minor semi-axis of 98.06 meters. In the olive grove's IDW the power parameter selected was also 2 with an 8 sector type neighbourhood type. The maximum and minimum neighbours selected were the ones that optimized the respective model, 10 and 15. An 8 sector type was selected with a major and minor semi-axis of 382 meters. The magnitude of the RMSE values did not change much, so more emphasis was placed in obtaining unbiased prediction with a mean error close to zero.

3.6 Kriging Interpolation

Ordinary Kriging was used as a geostatistical procedure to generate an estimated surface from a scattered set of points with the mean NDVI values. In line with the undertaken exploratory spatial data analysis, it was possible to conclude that there was no evidence of an anisotropic pattern for the whole data set area, so it was assumed isotropy, for both variables. The corresponding omnidirectional experimental variograms were modelled, according to the characteristics of the variables. The Average Nearest Neighbour tool was used to determine the average distance between points and their nearest neighbours to be used in the lag size. The values used in the lag size were 2 meters for the vineyard and 4 meters for olive grove. A good fit was obtained with the range value around 20 meters for the vineyard and 40 for the olive grove. The sill

selected was the default value and the nugget was enabled for the olive grove model. For the vineyard was used a k-bessel model with a parameter of 0.47, while in the olive grove a Gaussian model was used. The models selected were the ones considered to better fit the experimental variograms. The neighbourhood parameters' values were tested with the objective of reducing the associated errors of the two interpolations. Results achieved and parameters tested are shown in Figure 25, chapter 4.6.

4 RESULTS

4.1 UAV Imagery Collection and Processing

In Table 2. is presented the quality check report from the image collection and processing stages. Enough visual content could be extracted from the images with more than 10000 points extracted per image.

Quality Check per Flights

Quality Check	RGB Olive	MS olive	RGB Vine	MS vine
Images - Median of Key Points per Image	72233	10000	70494	10000
Dataset - Images Calibrated	1438 - 99%	2188 - 100%	1258 - 99%	4660 - 100%
Camera Optimisation - Relative Difference Initial and Optimised internal Camera Parameters	0,66%	0,08%	0,23%	0,06%
Matching - Median Matches per Calibrated Image	43245,2	5274,5	18802,1	5670,85

*MS – Multispectral

Table 2. Quality check report.

At least 99% of the images were calibrated in a single block for each flight.
The maximum percentage of the difference between initial and optimized focal

length in all flights were 0,66% and more than 5000 matches have been computed per calibrated image.

4.2 Vine Classification

4.2.1Principal Components Analysis

In Table 3. is the correlation matrix of PC's Analysis for the vineyard study area. It shows high correlation between the RGB bands and between the Multispectral bands.

CORRELATION MATRIX VINE TREE PC ANALYSIS

	DEM Diff	R	G	B	NDVI	GNDVI
Layer	**1**	**2**	**3**	**4**	**5**	**6**
1		-0,33	-0,29	-0,33	0,43	0,33
2	-0,33	1,00	0,99	0,99	-0,53	-0,37
3	-0,29	0,99		0,99	-0,49	-0,36
4	-0,33	0,99	0,99	1,00	-0,52	-0,37
5	0,43	-0,53	-0,49	-0,52		0,76
6	0,33	-0,37	-0,36	-0,37	0,76	1,00

Table 3. Correlation Matrix vine PC Analisys.

From Table 4., listing the principal components and the respective Eigenvalues percentage, is possible to see that three principal components were enough to explain more than 97% of variance present in the data. It important to take in consideration that both NDVI and GNDVI were calculated using the bands from the Multispectral sensor and not the red or green band from the RGB camera.

PRINCIPAL COMPONENT VINE TREE CLASSIFICATION

Layer	EigenValue	Percent of EigenValues	Accumulative of EigenValues
1	4223,93001	75,6019	75,6019
2	810,20008	14,5013	90,1032
3	438,50793	7,8486	97,9519
4	114,43087	2,0481	100,0000

Table 4. Principal Components vine classification.

The polygon's size distribution resulting from the classification phase was analysed and is depicted in the histogram in Figure 9 with the range of values separated into 10 classes with a logarithm transformation. The histogram indicates that the data is bimodal and asymmetric. The left tail of the distribution shows the presence of many polygons with low area sizes.

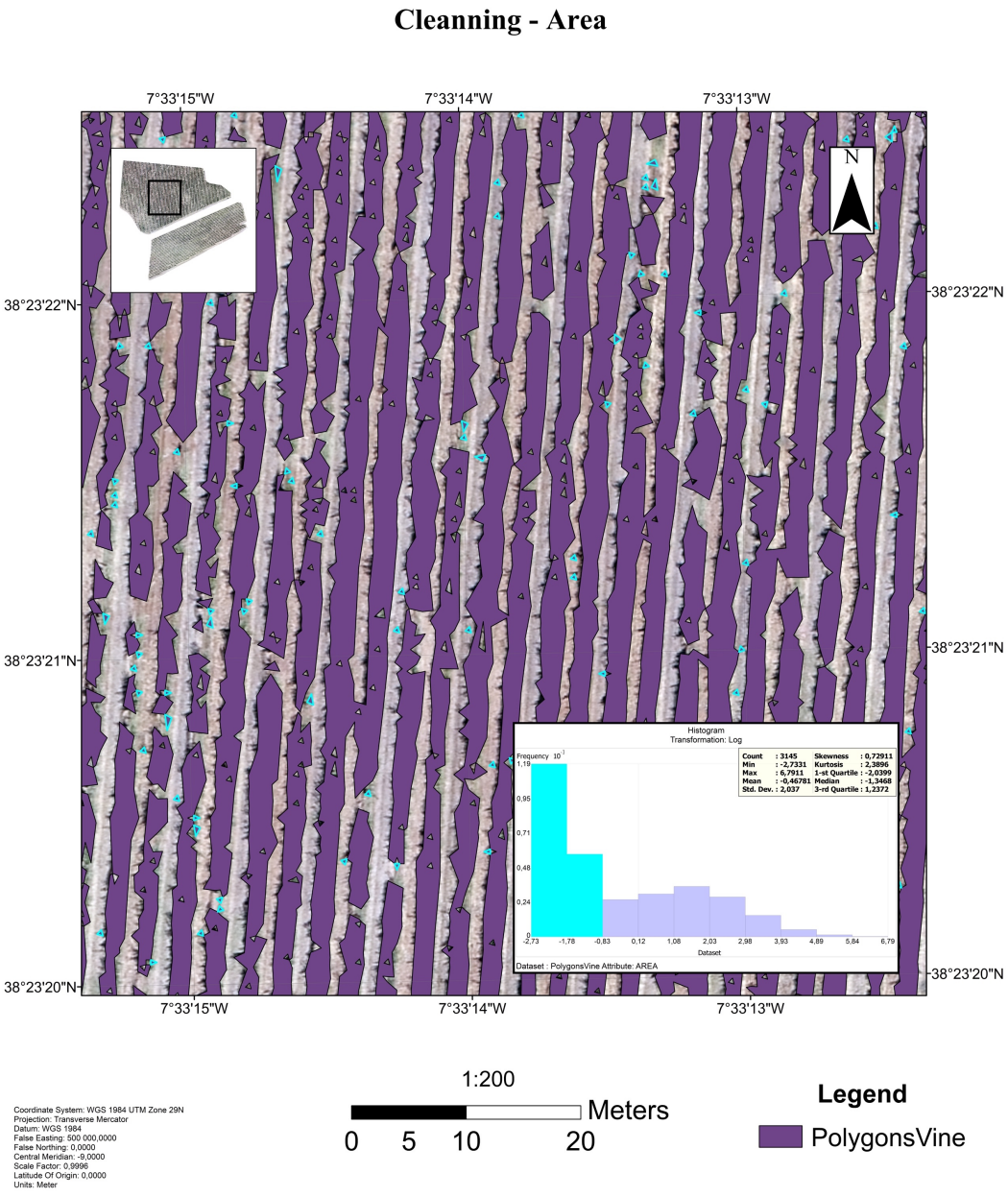

Figure 9. Classified polygons and cleanning selection for the vineyard.

In Figure 9. are selected the two bars in the distribution corresponding to the polygons with lowest areas that were not considered for the analysis. It was possible to see that due to their size they were not indicating vines, rather they were representing in their majority weeds and other objects, causing processing

problems. These Polygons with smaller areas (<0,1479 m2) were selected using the histogram representing the size of the polygons and their distribution. This selection of polygons was not considered for the rest of analysis, resulting in a unimodal distribution.

4.2.2Outlier and Cluster Analysis

For the mean NDVI point data the Spatial Autocorrelation by Distance graphic (Figure 10.) exhibits a single peak at 95 meters so the Distance Band or Threshold Distance parameter was set to 100 meters for the vineyard study area.

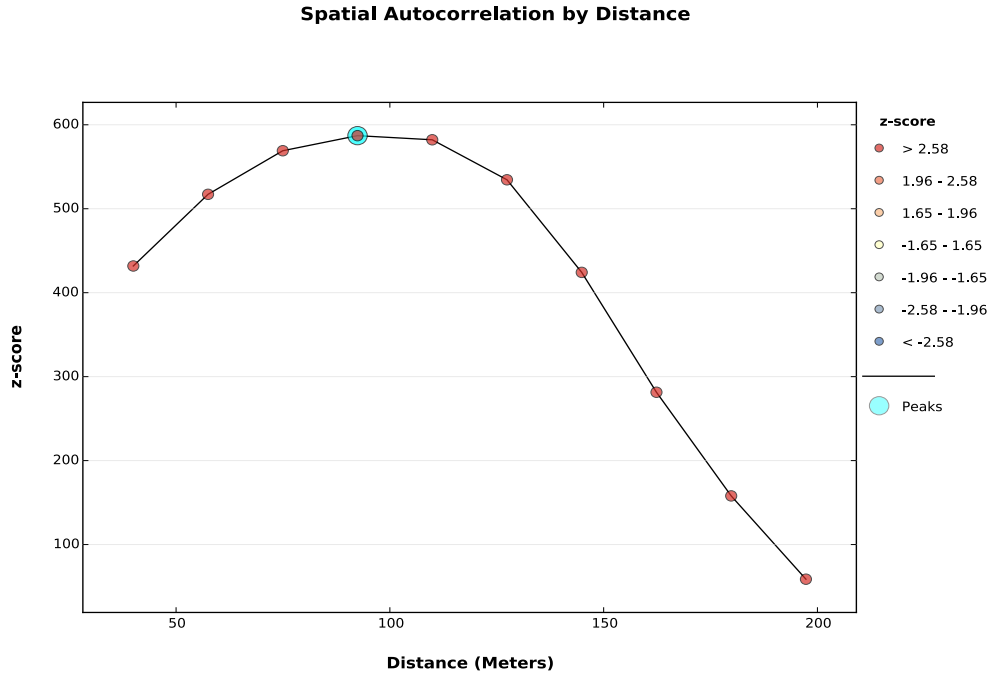

Figure 10. Vineyard's Spatial Autocorrelation by distance graph.

For the vineyard mean NDVI data, the Global Moran's I value equals to 0.63 and it is statistically significant (p-value<0.05) (Figure 11), which provides evidence that the spatial distribution of high values and/or low values in the dataset is more spatially clustered than would be expected if related spatial processes were random. When analysing the Ansellin's Local Moran's I map, Figure 11. is possible to identify a cluster of high values located in the north eastern corner of the study area and a cluster of low values located both in the western side and in the south corner of the vineyard. The remaining points were not statistically significant, meaning that there is not enough evidence to reject

the complete spatial randomness hypothesis with 95% confidence. Results also show that there is presence of spatial outliers (Figure 11.), these points were not considered for the Interpolation stage.

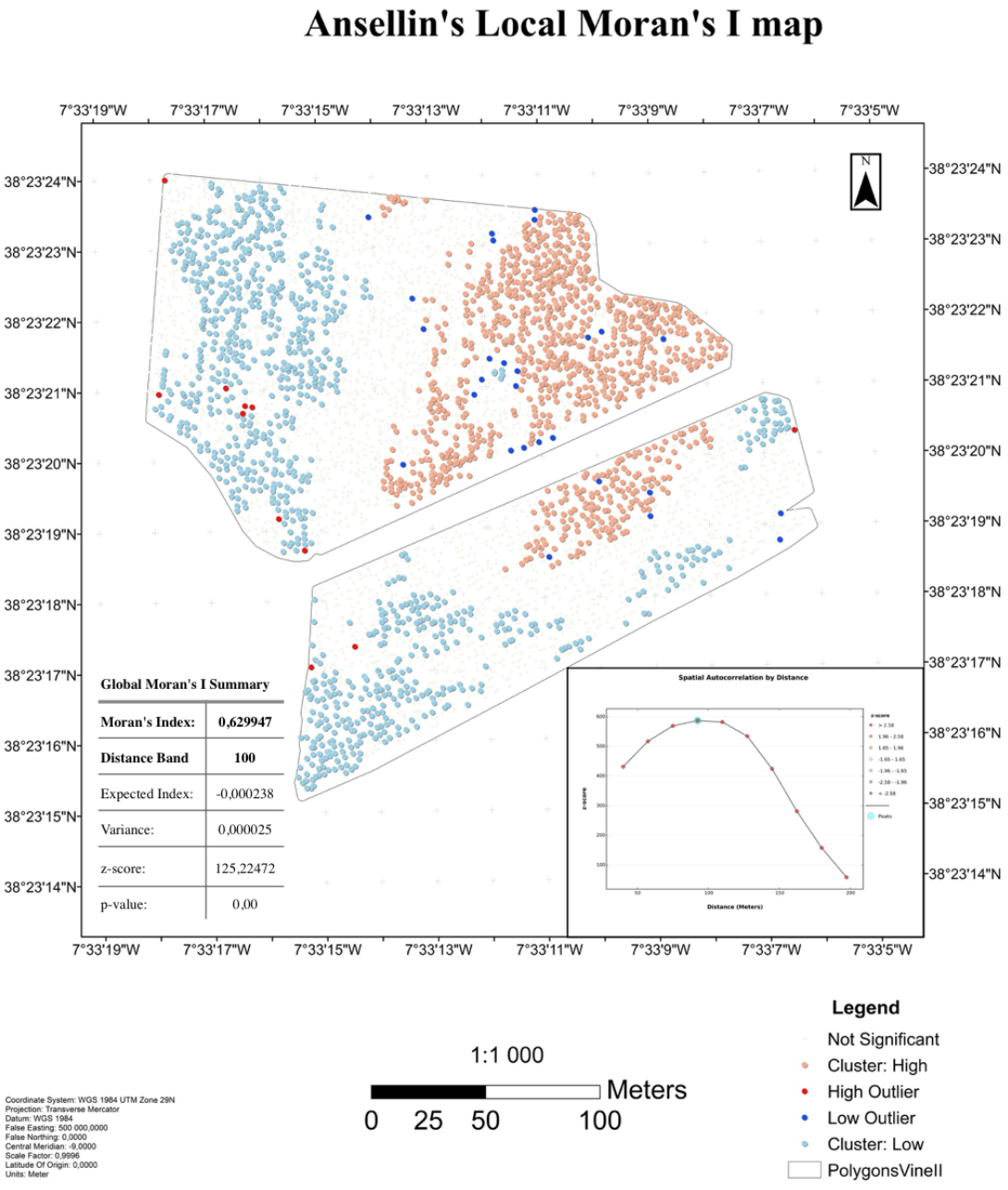

Figure 11. Ansellin's local Moran's I map for the vineyard.

4.3 Olive tree Classification

4.3.1Principal Components Analysis and ISO Cluster Analysis

In Table 5. is presented the correlation matrix of PC's Analysis for the olive grove. Consistent with previous results it shows high correlation between the different RGB bands and between the Multispectral bands. An important aspect to take in consideration is that both NDVI, GNDVI and NDRE were calculated using the bands from the Multispectral sensor and not the red or green band from the RGB camera.

CORRELATION MATRIX OLIVE TREE PC ANALYSIS

	NDRE	GNDVI	NDVI	DEM Diff	R	G	B
Layer	**1**	**2**	**3**	**4**	**5**	**6**	**7**
1		0,58	0,66	0,23	-0,43	-0,39	-0,44
2	0,58		0,88	0,11	-0,37	-0,31	-0,40
3	0,66	0,88		0,12	-0,41	-0,33	-0,42
4	0,23	0,11	0,12		-0,17	-0,18	-0,17
5	-0,43	-0,37	-0,41	-0,17		0,98	0,95
6	-0,39	-0,31	-0,33	-0,18	0,98		0,97
7	-0,44	-0,40	-0,42	-0,17	0,95	0,97	

Table 5. Correlation Matrix olive tree PC Analisys.

From Table 6., listing the principal components and the respective Eigenvalues percentage, is possible to see that, just like in the vineyard case, three principal components were enough to explain more than 97% of variance present in the data.

Layer	EigenValue	Percent of EigenValues	Accumulative of EigenValues
1	1625,30	70,38	70,38
2	558,33	24,18	94,56
3	62,36	2,70	97,26
4	39,72	1,72	98,98
5	23,63	1,02	100,00

Table 6. Principal Components olive grove classification.

The polygon's size distribution resulting from the classification phase was analysed and is depicted in the histogram in Figure 12. with the range of values

separated into 10 classes with a logarithm transformation. The histogram indicates that the data is bimodal and asymmetric. The left tail of the distribution shows the presence of a many polygons with low area sizes, just like the vineyard case.

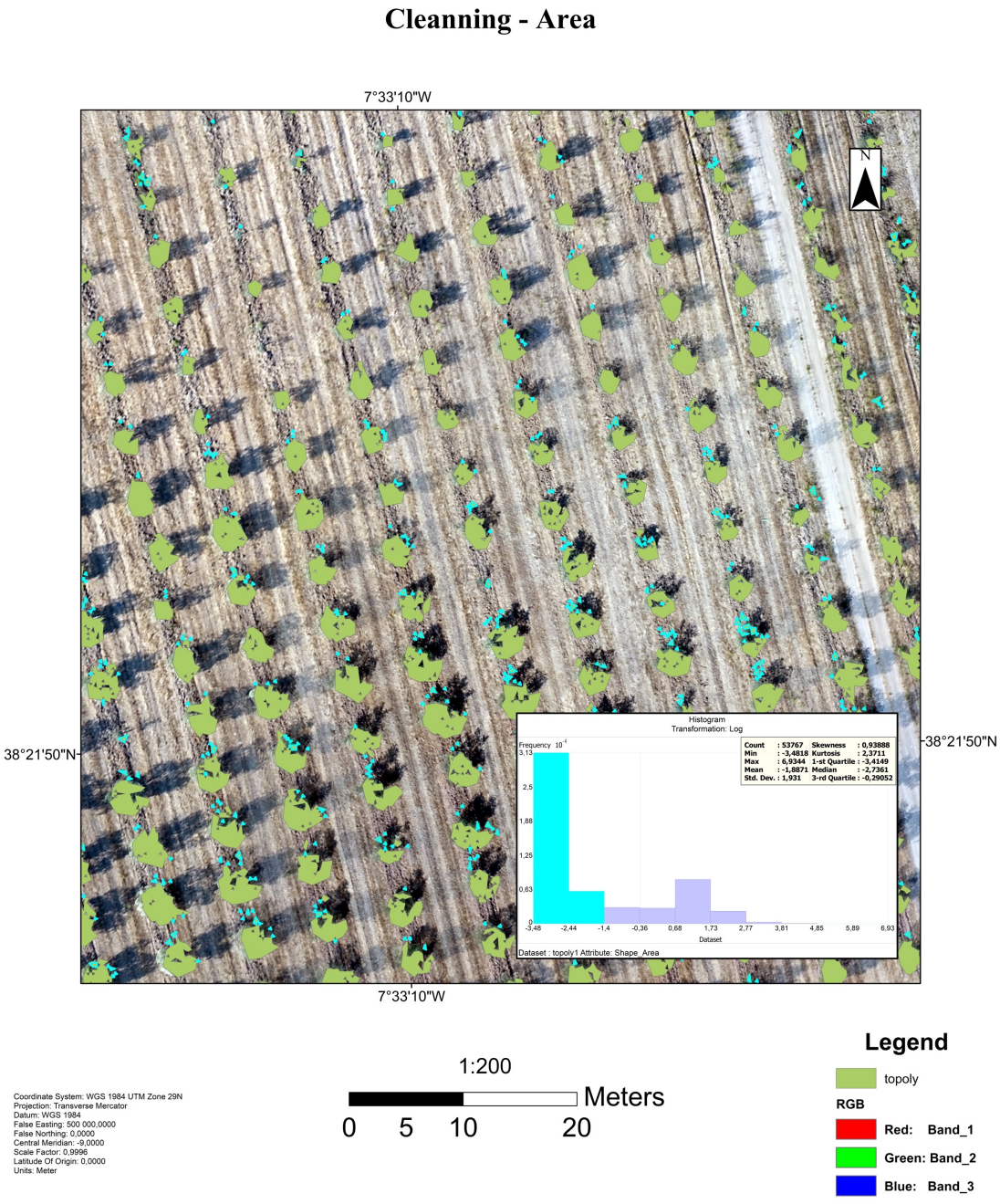

Figure 12. Classified polygons and cleanning selection for the olive grove.

In Figure 12. are selected the two bars in the distribution corresponding to the olive tree polygons with lowest areas that were not considered for the analysis. It is possible to see that due to their size they were not indicating vines, rather

they were representing in their majority weeds and other objects, causing processing problems. These Polygons with smaller areas (<0,0398 m2) were selected using the histogram representing the size of the polygons and their distribution. This selection of polygons was not considered for the rest of analysis, resulting in a unimodal distribution.

4.3.2Outlier and Cluster Analysis

For the mean NDVI point data the Spatial Autocorrelation by Distance graphic (Figure 13.) exhibits a first peak at 505 meters, thus the *Distance Band* or *Threshold Distance* parameter was set to 500 meters.

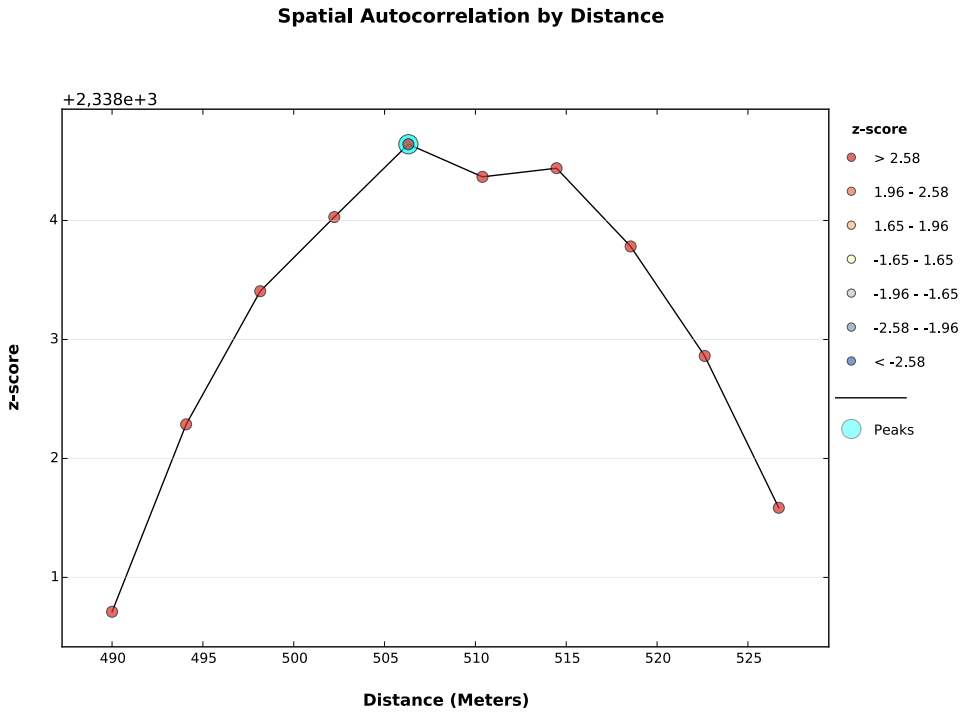

Figure 13. Olive grove's Spatial Autocorrelation by distance graph.

For the olive grove mean NDVI data, the Global Moran's I value equal to 0.50 and it is statistically significant (p-value<0.05) (Figure 14.), which provides evidence that the spatial distribution of high values and/or low values in the dataset is more spatially clustered than would be expected if related spatial processes were random. When analysing the Ansellin's Local Moran's I map, Figure 14. is possible to identify a cluster of high values located in the western side of the olive grove and a cluster of low values located in the eastern side of the olive grove. This distinct clustered pattern is suspected to be caused by a

temporal interval in the year the olive trees were planted causing this clustering pattern in the mean NDVI data. There is also the possibility of different species being present in the olive grove study area. The remaining points are not statistically significant, meaning that there is not enough evidence to reject the 'complete spatial randomness' hypothesis with 95% confidence. Results show also that there is presence of spatial outliers (Figure 14.), thus these points were not considered for further analysis. Note that the maximum distance allowed by the processing capabilities available was 400 meters.

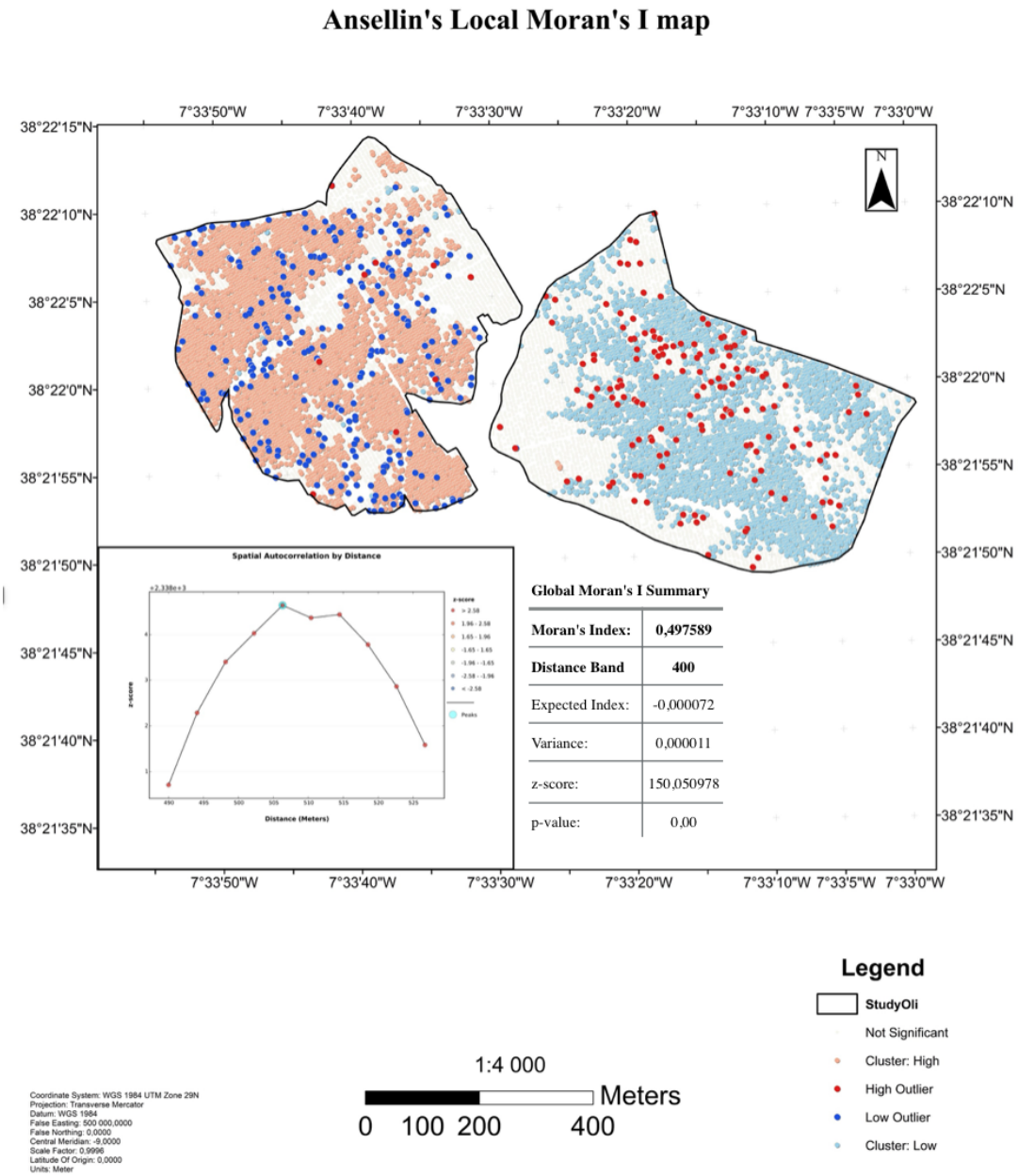

Figure 14. Ansellin's local Moran's I map for the olive grove.

4.4 Exploratory Spatial Point Data Analysis

With the NDVI point data created, the map of graduated colours provides an insight on the spatial distribution of the mean NDVI values (Figure 15). Descriptive statistics are also depicted in the upper-right corner of the Histogram.

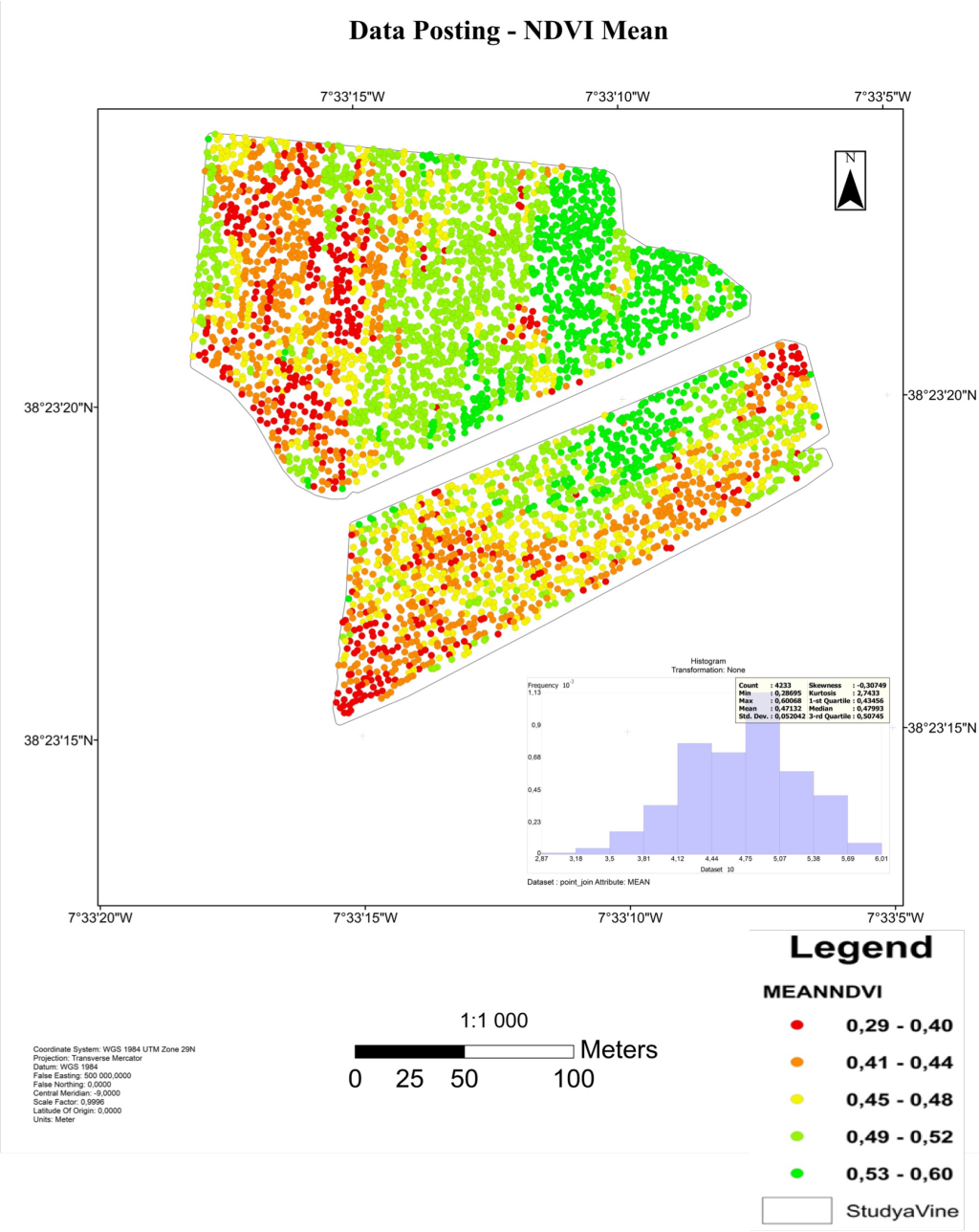

Figure 15. Point data posting.

For the vineyard, the highest values are located in the north eastern corner of the study area. The lowest values are located both in the western side and in

the south corner of the vineyard. The distribution of the mean NDVI values is depicted in the histogram (Figure 15.) with the range of values separated into 10 classes. The frequency of data within each class is represented by the height of each bar. The histogram indicates that the data is unimodal and nearly symmetric. Descriptive statistics for the vineyard shows that, there is an average of 1048 points per hectare, the regional average of the mean NDVI is equal to 0.47 and the typical deviation from this value is equal to 0.05.

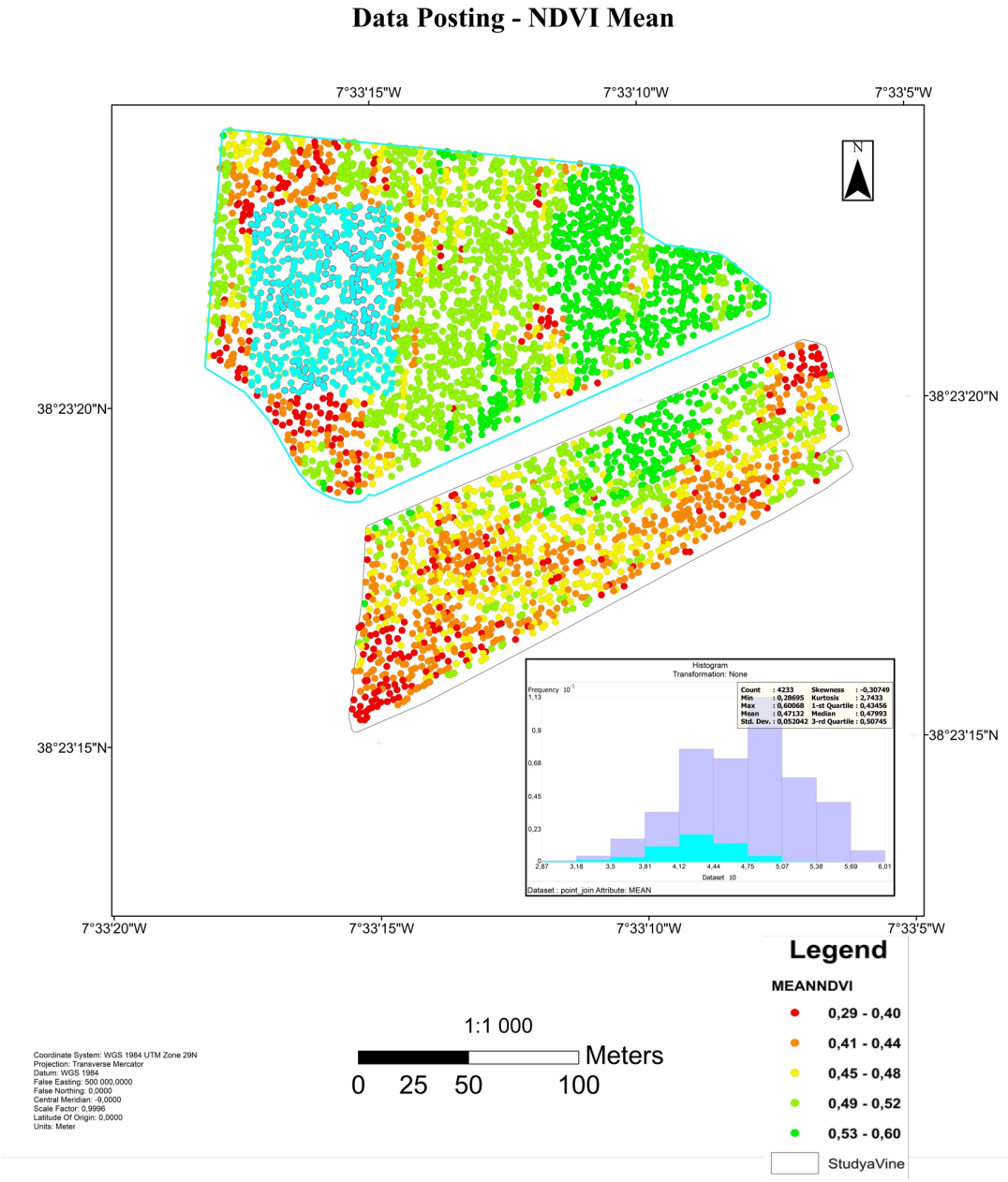

Figure 16. Lower Mean NDVI selection.

The mean NDVI is smaller than 0.48 in 50% of the points. An area with lower mean NDVI values was selected with the objective of investigating spatial regimes. The bars corresponding to the selected observations are depicted in the histogram (Figure 16.) this functionality is suitable to examine the possible presence of spatial regimes, however the points in this area are spread throughout the histogram, thus there is no evidence of a proportional effect in the area selected.

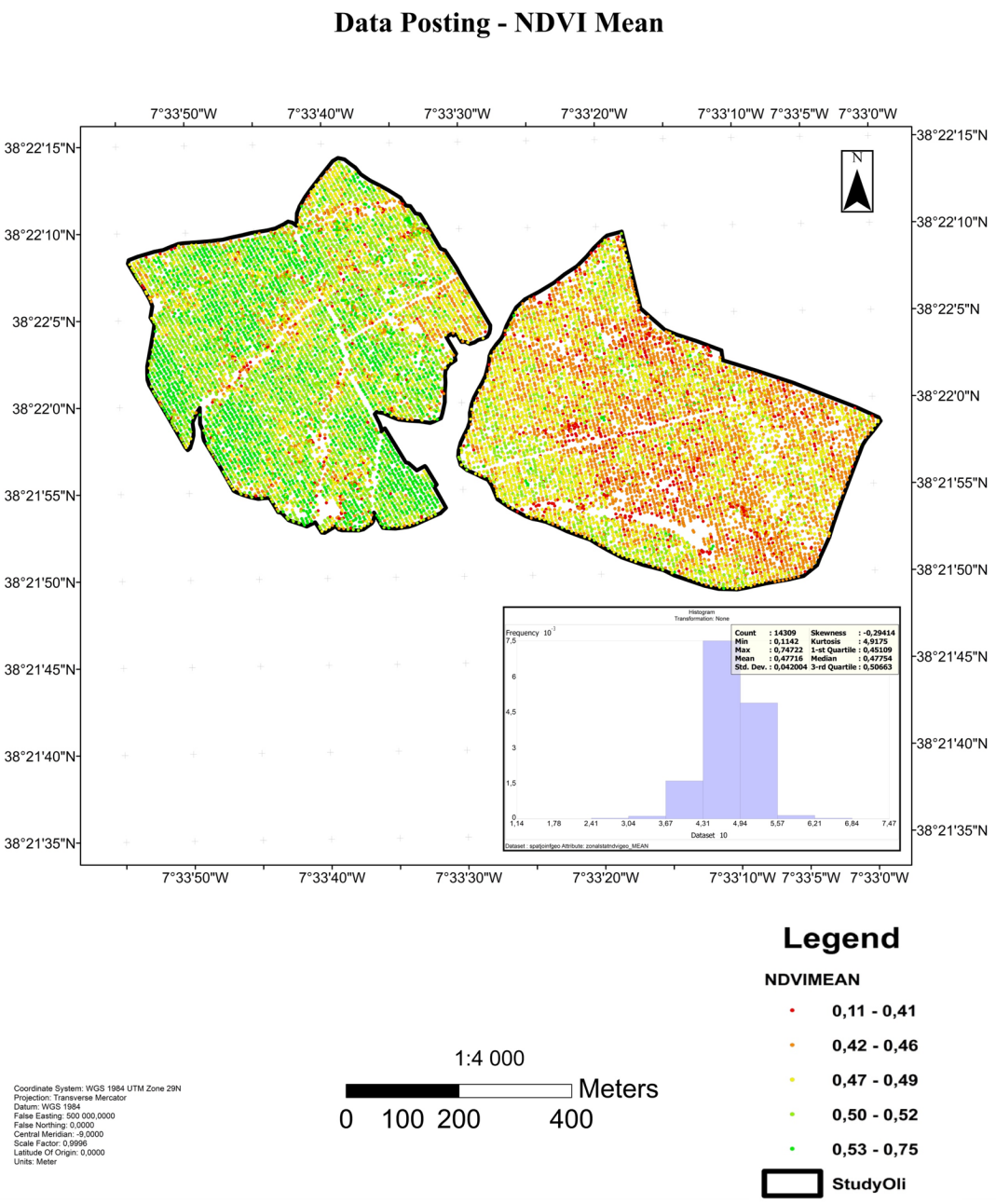

Figure 17. Point data posting.

For the Olive grove, the highest values are located in the western side of the olive grove. (Figure 17.) The lowest values are located in the eastern side of the olive grove, it is suspected that it could be caused by a temporal interval in the year which the olive trees were planted causing this pattern in the mean NDVI data. There is also the possibility of different species being present in the olive grove study area. The distribution of the mean NDVI values is depicted in the histogram (Figure 17.) with the range of values separated into 10 classes. The frequency of data within each class is represented by the height of each bar.

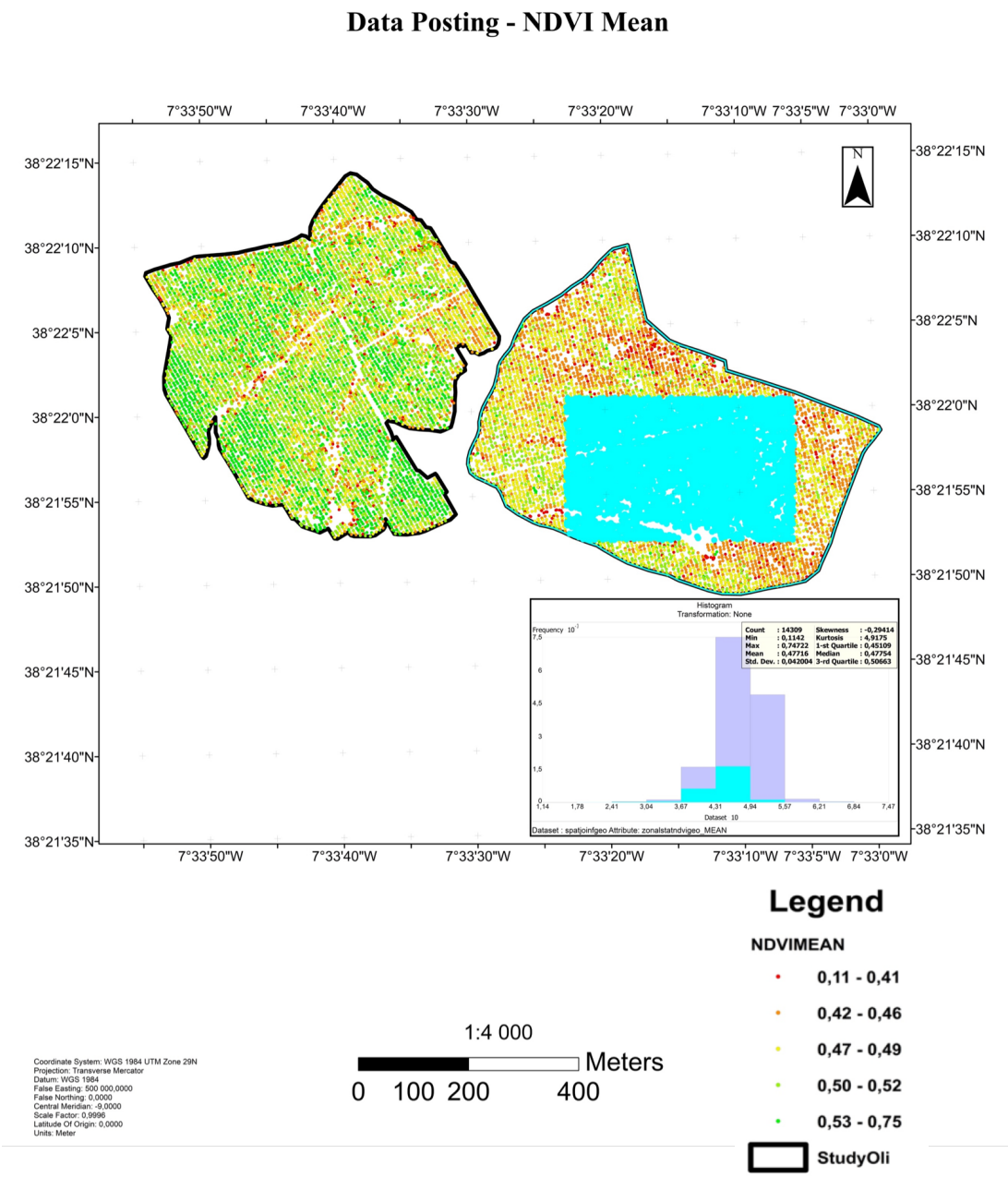

Figure 18. Lower Mean NDVI selection.

The histogram indicates that the data is unimodal and approximately symmetric just like in the vineyard case. The descriptive statistics for the olive grove shows that, the mean NDVI was measured in 14309 points and there is an average of 271 points per hectare. In the olive grove case this number can be used to estimate the number of olive trees planted in the olive grove. The regional average of the mean NDVI is equal to 0.47, and the typical deviation from this value is equal to 0.04. The mean NDVI is smaller than 0.48 in 50% of the points. An area with lower Mean NDVI values was also selected with the objective of investigating spatial regimes. The bars corresponding to the selected observations are depicted in the histogram (Figure 18.) with the objective of examine the possible presence of spatial regimes in the olive grove point data, however the points in this area are spread throughout the histogram, thus there is no evidence of a proportional effect in the area selected.

4.5 Inverse Distance Weighted Interpolation

VINEYARD SEARCHING NEIGHBOURHOOD

Sector type	Min neighbourhood	Max neighbourhood	Mean error	RMSE
4 Sector	3	8	0,000351	0,021714
4 Sector	5	10	0,000355	0,021840
8 Sectors	10	15	0,000359	0,022720
4 Sector	5	10	0,000361	0,022135
4 Sectors with 45° offset	10	15	0,000387	0,022127

OLIVE GROVE SEARCHING NEIGHBOURHOOD

Sector type	Min neighbourhood	Max neighbourhood	Mean error	RMSE
8 Sector	10	15	-0,000988	0,027769
8 Sector	15	20	-0,000993	0,027772
4 Sector	10	15	-0,001003	0,027827
4 Sectors with 45° offset	10	15	-0,001006	0,027820
1 Sector	10	15	-0,001041	0,028388

Table 7. Searching neighbourhood table.

The IDW prediction errors achieved were low and near zero for both study areas, which suggests unbiased prediction errors. (Table 7.) The mean square error (MSE) recorded for the vineyard was 0,022 and for the olive grove 0,028. In the first rows are represented the parameters selected to the final models.

Figure 19., 20., 21. and 22. show the predicted surface with graduated colours and contour line of the mean NDVI data, which was obtained using IDW with the best search neighbourhood definitions in Table 7. In the vineyard, the predicted surface and contour line map of the mean NDVI data (Figure 19. and 20.) neither exhibited an overall anisotropic pattern nor a global trend.

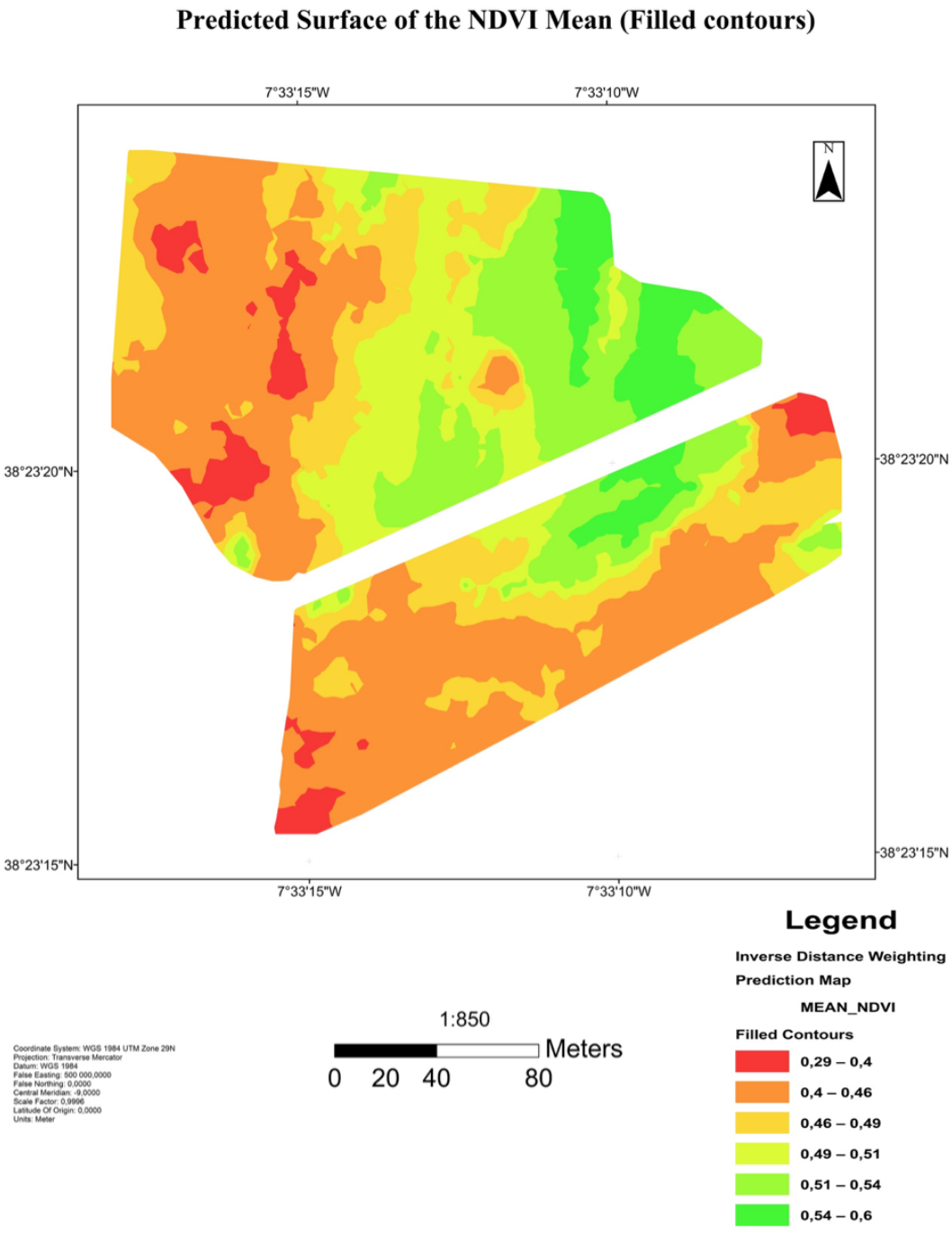

Figure 19. Vineyard predicted surface

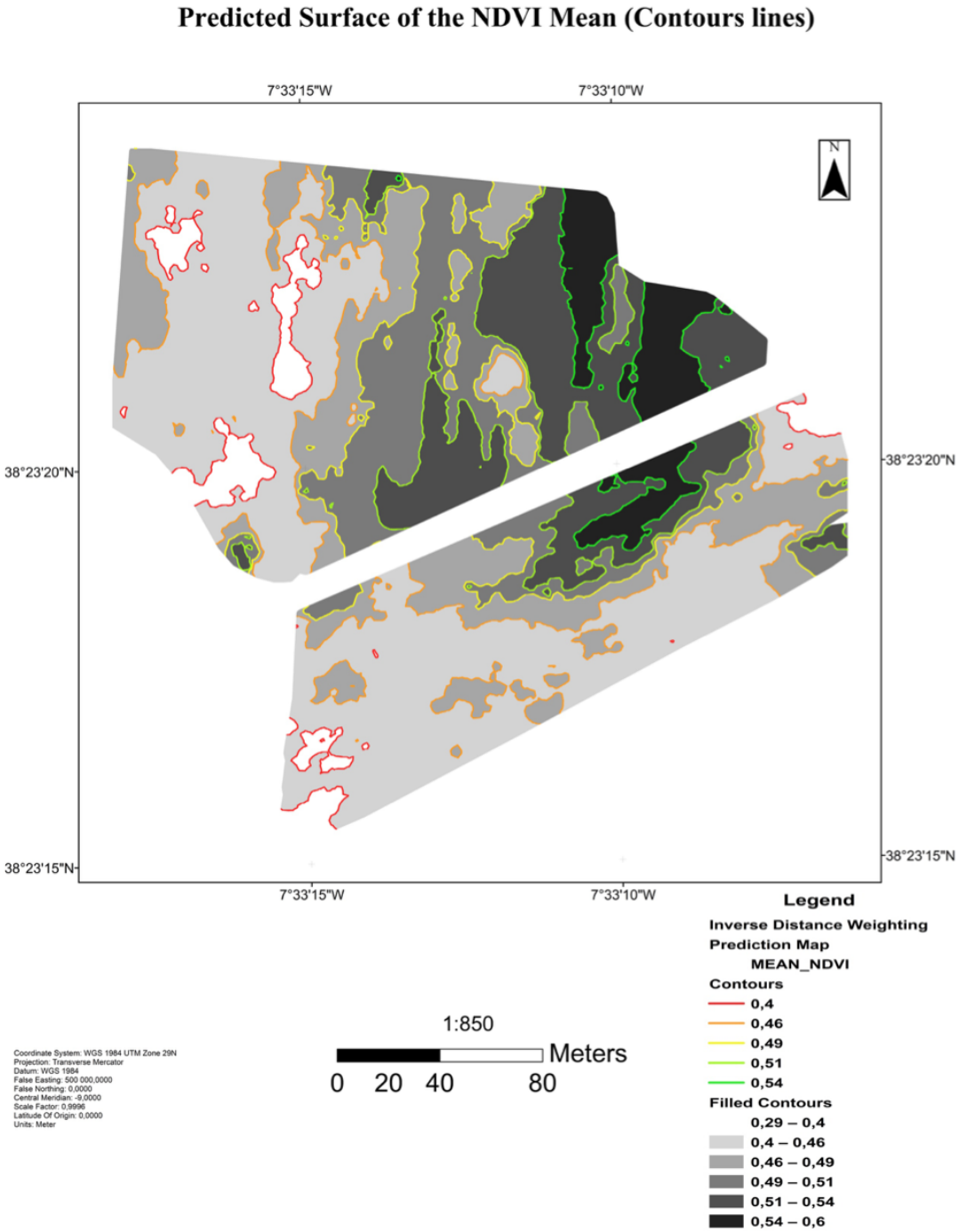

Figure 20. Vineyard contour lines map.

In the olive grove the predicted surface and contour line map of the mean NDVI data (Figure 21. and 22.) also did not exhibit an overall anisotropic pattern but is possible to notice a small trend between the right and left side of the olive grove, probably explained by the different ages of the olive trees present in the study area.

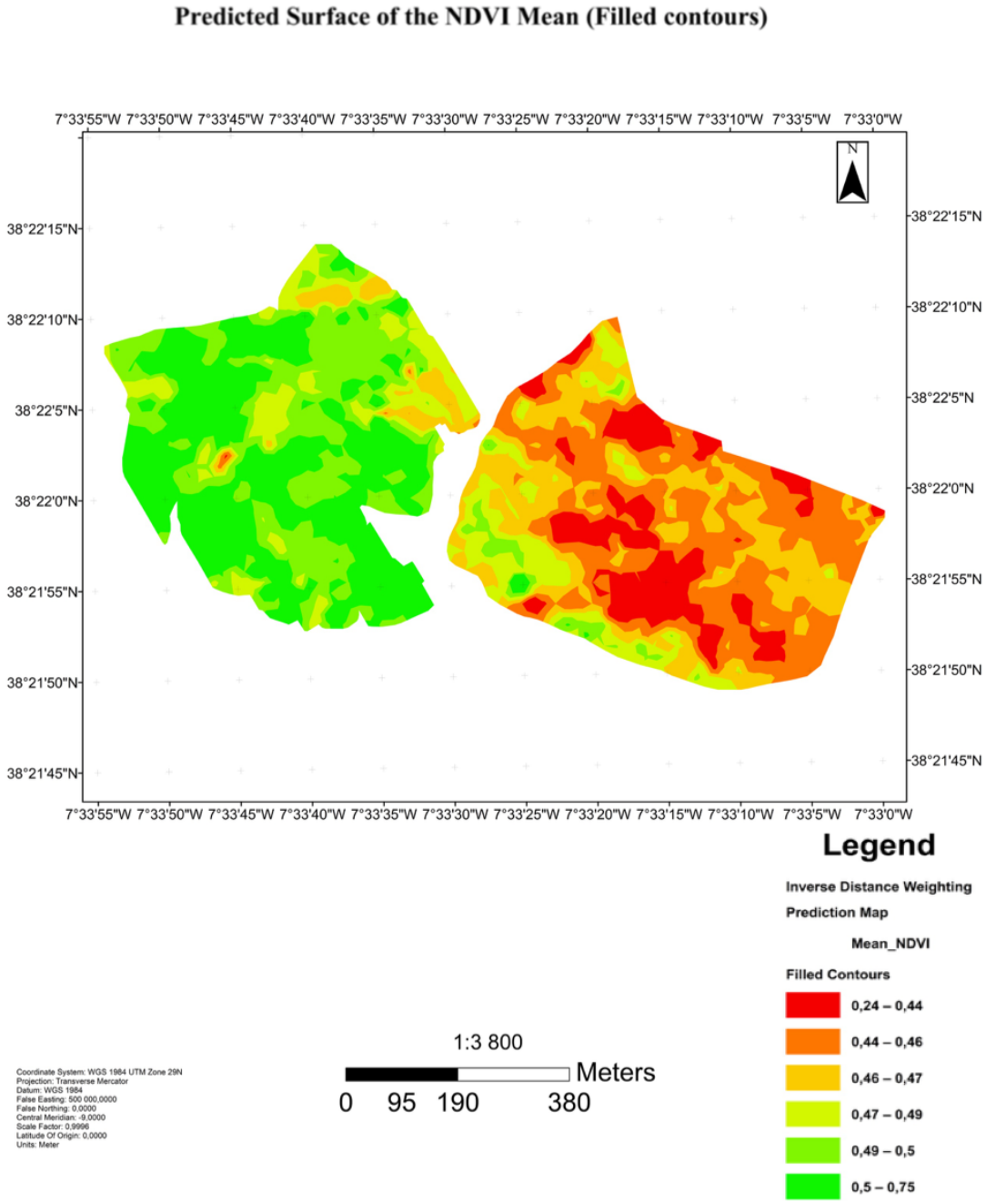

Figure 21. Olive grove predicted surface.

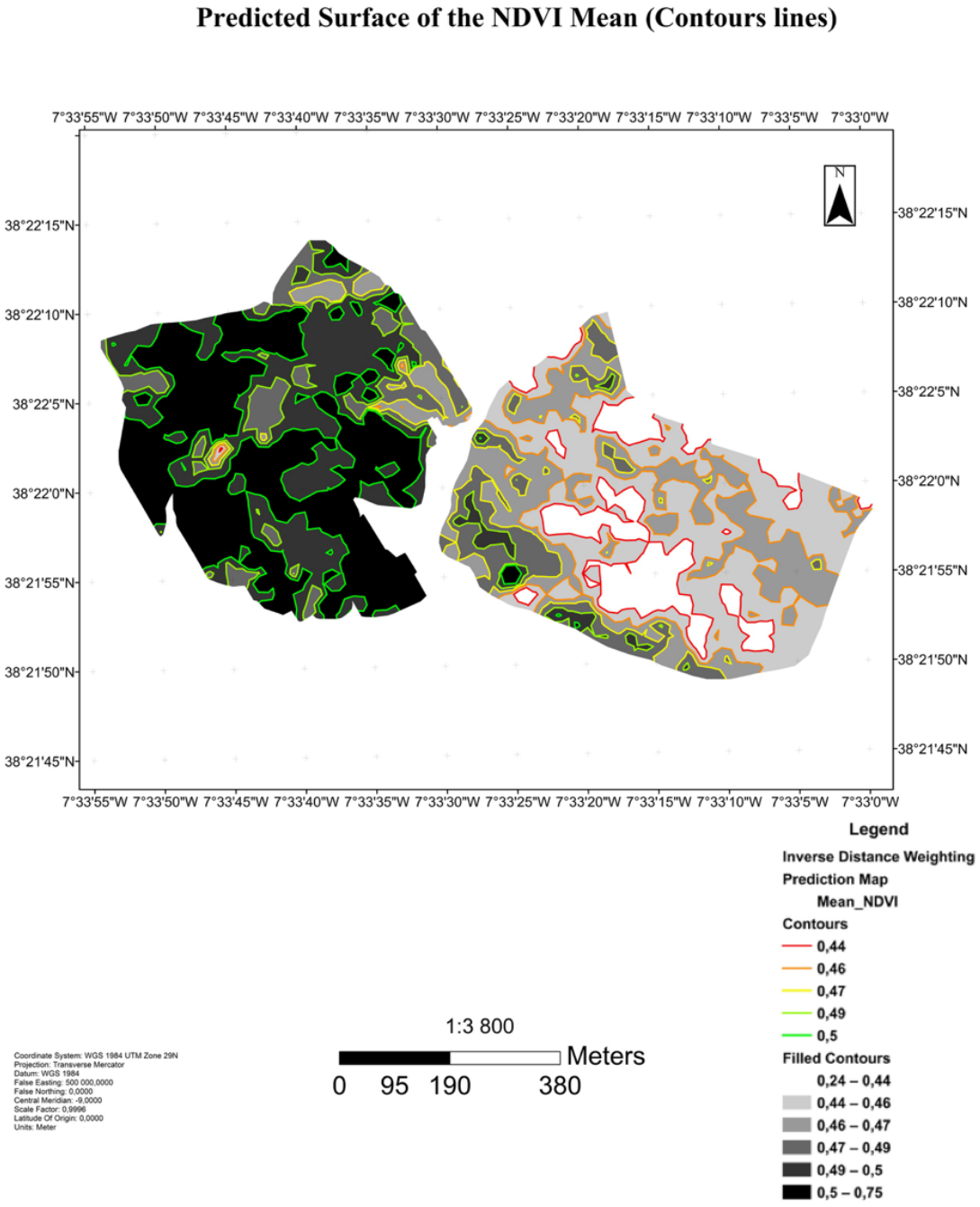

Figure 22. Olive grove contour lines map.

The mean and local standard deviation maps of the mean NDVI data are presented in Figure 23. and 24. The local standard deviation maps exhibit a larger concentration of high values in locations where the local mean exhibits low values of mean NDVI, this is particularly clear in the vineyard study area. Consequently, there is evidence of a proportional effect over those areas, but because the areas in question are small, that effect was disregarded for the Kriging interpolation phase.

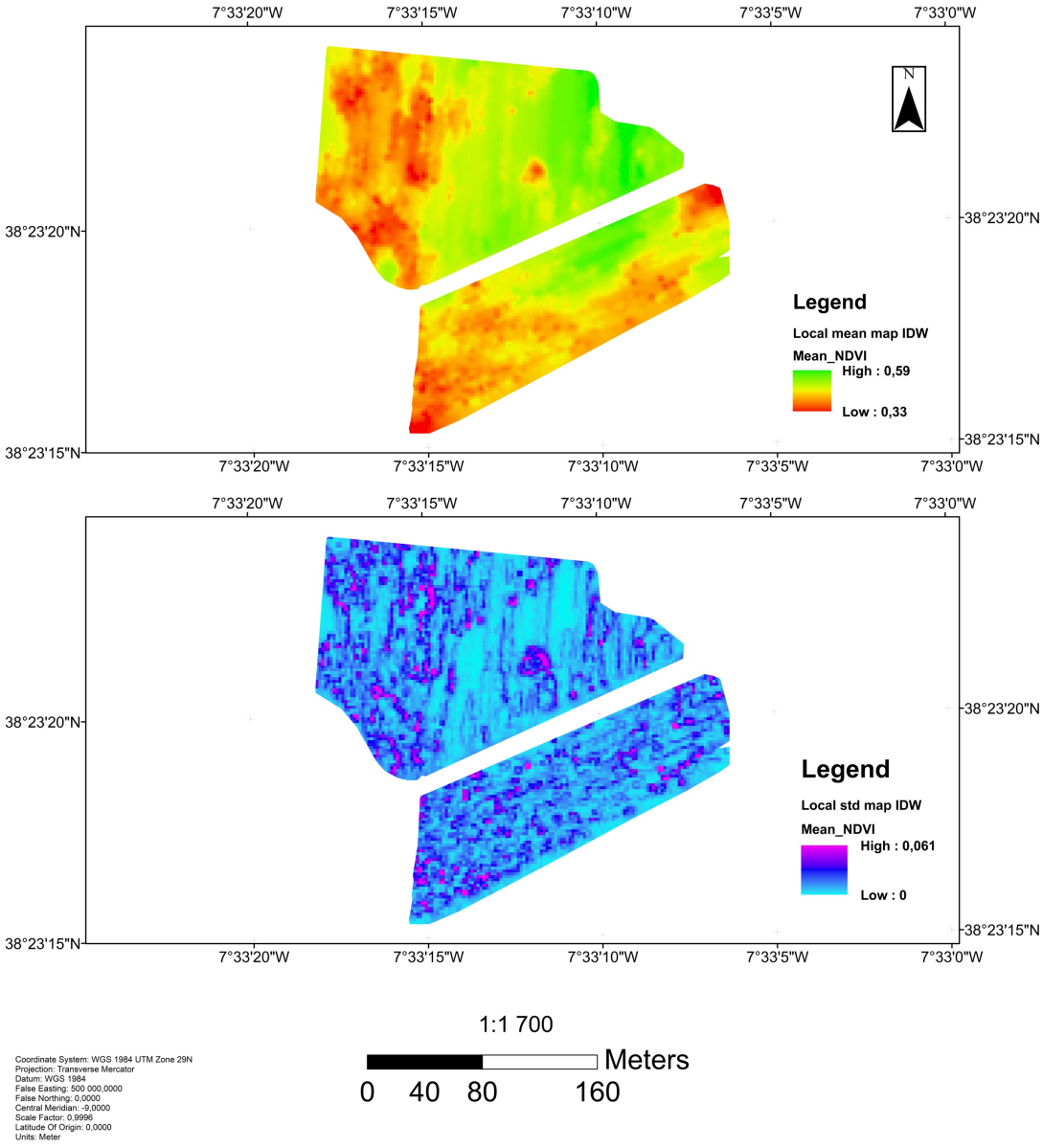

Figure 23. Mean and standard deviation maps of the mean NDVI data for the vineyard.

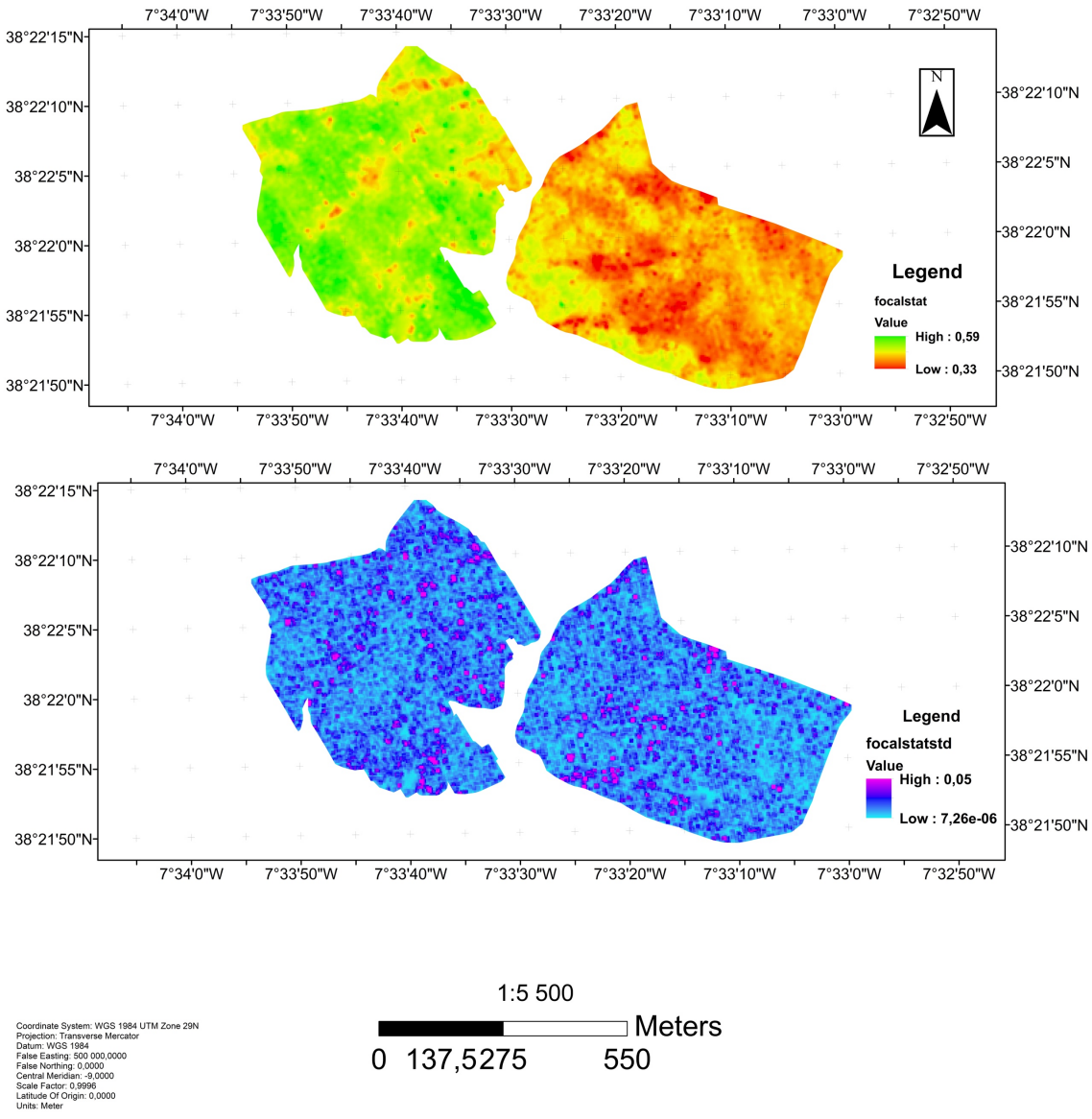

Figure 24. Mean and standard deviation maps of the mean NDVI data for the olivegrove.

4.6 Kriging Interpolation

In the first row of Figure 25. are represented the parameters selected to the final interpolation models.

OLIVE GROVE MODEL

Model Parameters	Gaussian
Nugget	0,000336
Major Range	40
Partial Sill	0,001319
Lag size	4
N. Lags	6

VINEYARD MODEL

Model Parameters	K-Bessel (0,474)
Nugget	0
Major Range	20
Partial Sill	0,0011
Lag size	2
N. Lags	10

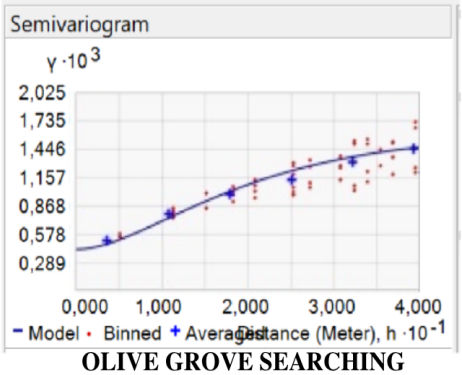

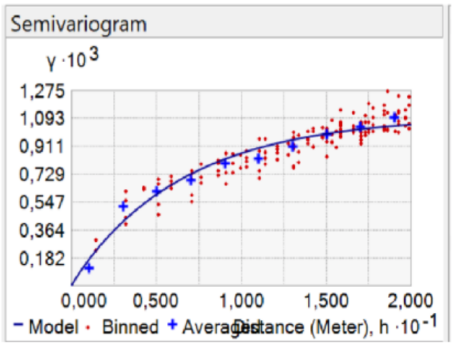

OLIVE GROVE SEARCHING

Sector type	Min neighbourhood	Max neighbourhood	Mean error	RMSE	RMSSE
4 Sectors with 45° offset	10	15	0,000076	0,031207	0,977079
4 Sectors with 45° offset	5	10	0,000084	0,031199	0,976640
8 Sector	2	5	0,000137	0,031192	0,976308
4 Sector	2	5	0,000150	0,031240	0,973979
4 Sectors with 45° offset	2	5	0,000169	0,031252	0,974378
1 Sector	2	5	-0,000375	0,032462	0,953804

VINEYARD SEARCHING NEIGHBOURHOOD

Sector type	Min neighbourhood	Max neighbourhood	Mean error	RMSE	RMSSE
4 Sector	2	5	0,000149	0,021227	1,088293
4 Sectors with 45° offset	2	5	0,000153	0,021246	1,089223
1 Sector	2	5	0,000262	0,023597	0,842425
8 Sector	2	5	0,000161	0,021231	1,088745

Figure 25. Kriging searching neighbourhood table and semivariogram.

The statistics in Figure 25. show that the mean errors achieved are low and the RMSSE's close to 1, with a mean error <0.001 in both cases, a RMSE of 0.031 for the vineyard and 0.021 for the olive grove and a RMSSE of 0.977 and 1.088, respectively. Figure 26. shows the predicted surface of the NDVI data for the vineyard, which was obtained using Ordinary kriging with the best search neighbourhood definitions specified in figure 25. In the vineyard (Figure 26.) it is explicit one large circular concentration of higher values in the Northeast part of the study area, other locations in the study area show some smaller concentrations of lower mean NDVI values, for example in the west side of the vineyard and in some locations in the southern area.

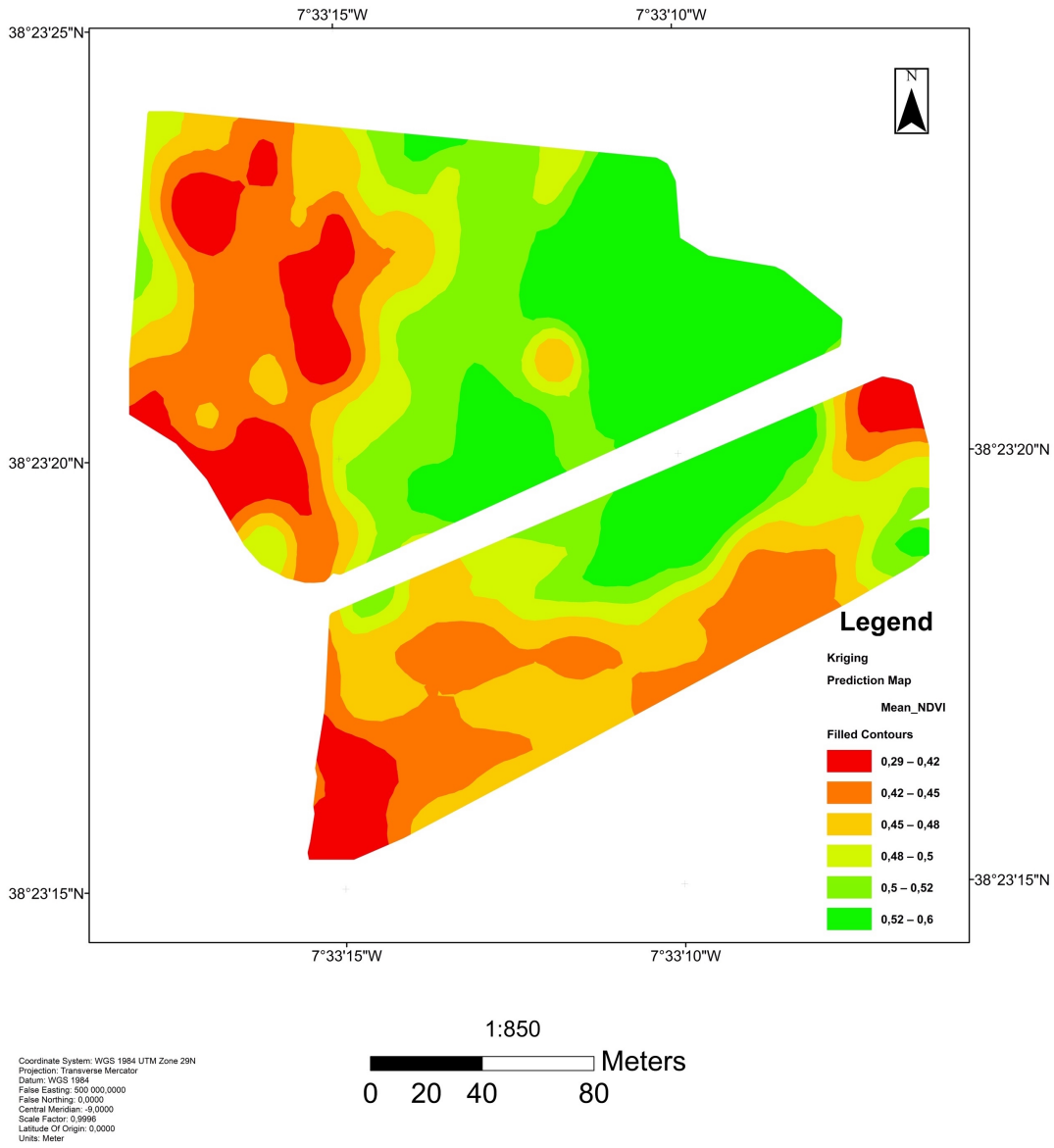

Figure 26. Predicted surface map.

The Prediction standard error map (Figure 27.) reflects data locations, this is a map of distance to the nearest NDVI point location scaled by the covariance function. In the Prediction standard error surface, locations with sample points show prediction standard errors equal to zero, since ordinary kriging is an exact interpolator. Locations near sample points show lower errors. So, this map can be useful to identify locations lacking data points. As it is possible to see there is not any concentration of high errors in the vineyard study area.

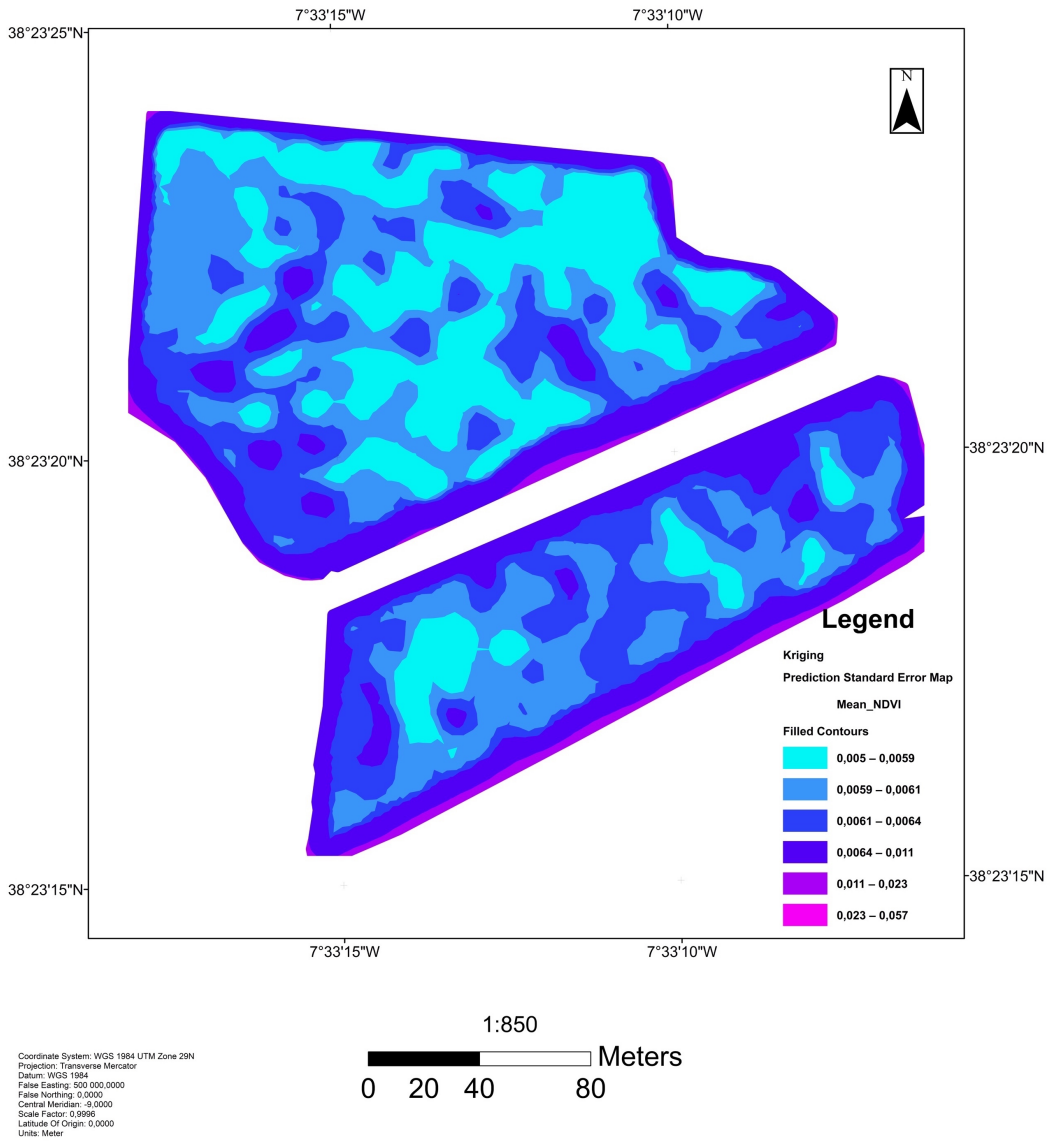

Figure 27. Prediction standard error map.

Figure 28. shows the predicted surface of the NDVI data for the olive grove, which was obtained using Ordinary kriging with the best search neighbourhood definitions specified in figure 25. In the olive grove (Figure 28.) it is clear the difference between the two sides, higher values in the west side of the study area and lower values in the eastern side, probably due to the presence of olive trees with different ages that would explain the difference between the two regions. In the Prediction standard error surface for the olive grove (Figure 29.), it is possible to perceive that there is not any concentration of high errors over the study area.

Predicted surface of the NDVI Mean (Filled Contours)

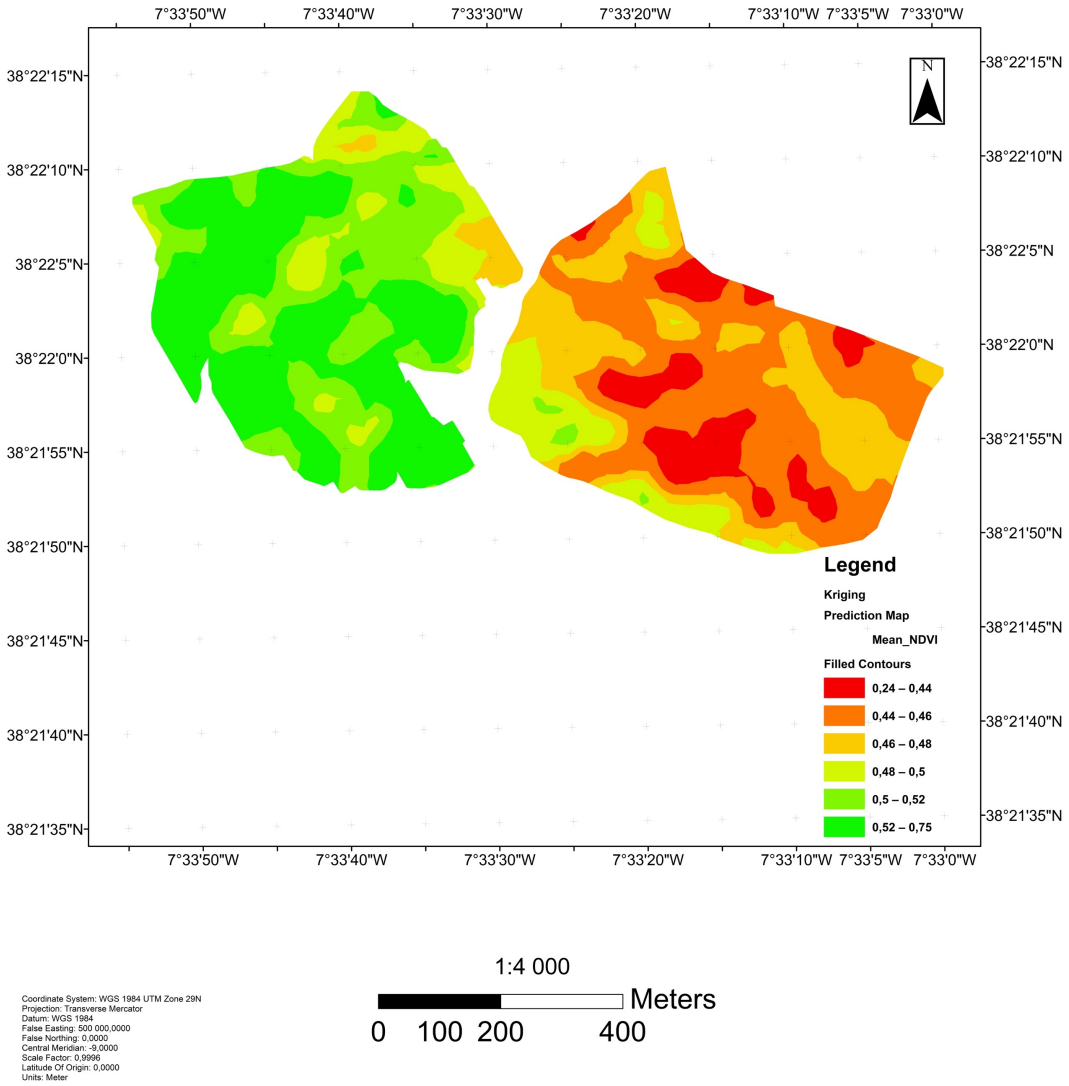

Figure 28. Predicted surface map.

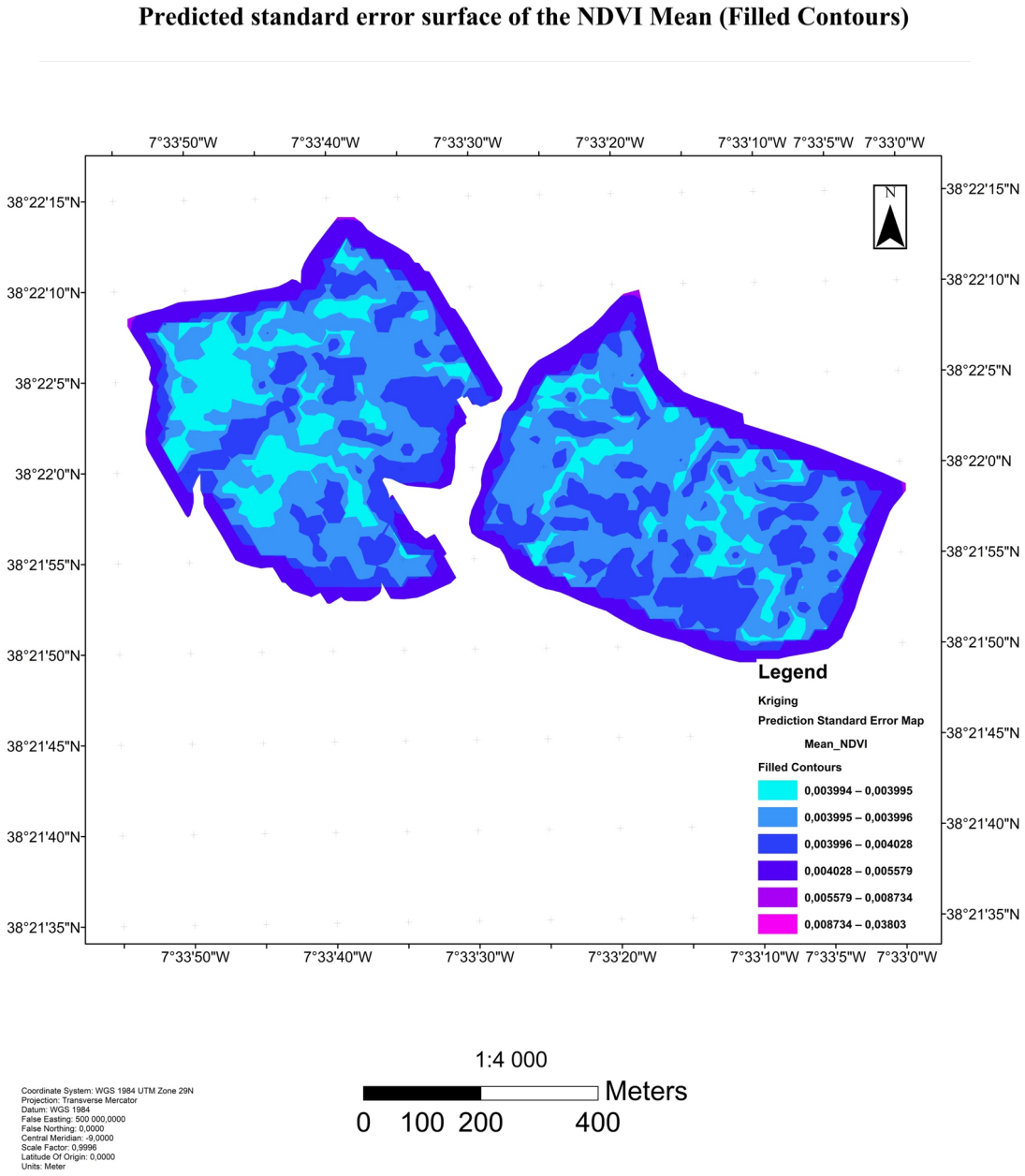

Figure 29. Prediction standard error map.

In Figure 30. And 31. are presented the original NDVI maps and as defined the final Vigor's Spatial Variability maps are presented in Figure 32. and 33. The predicted surfaces were exported to a simplified raster format with a 2 and 3 meters' pixel size just for visualization proposes however other outputs can be created. The results show the true spatial variability present in the vegetation using the NDVI Index.

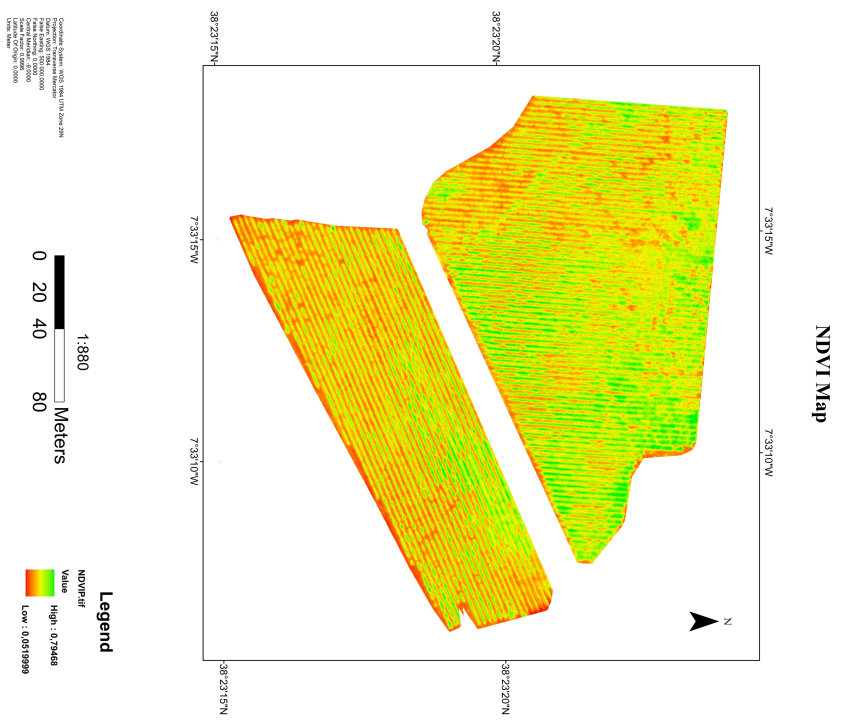

Figure 30. The original NDVI map for the vineyard.

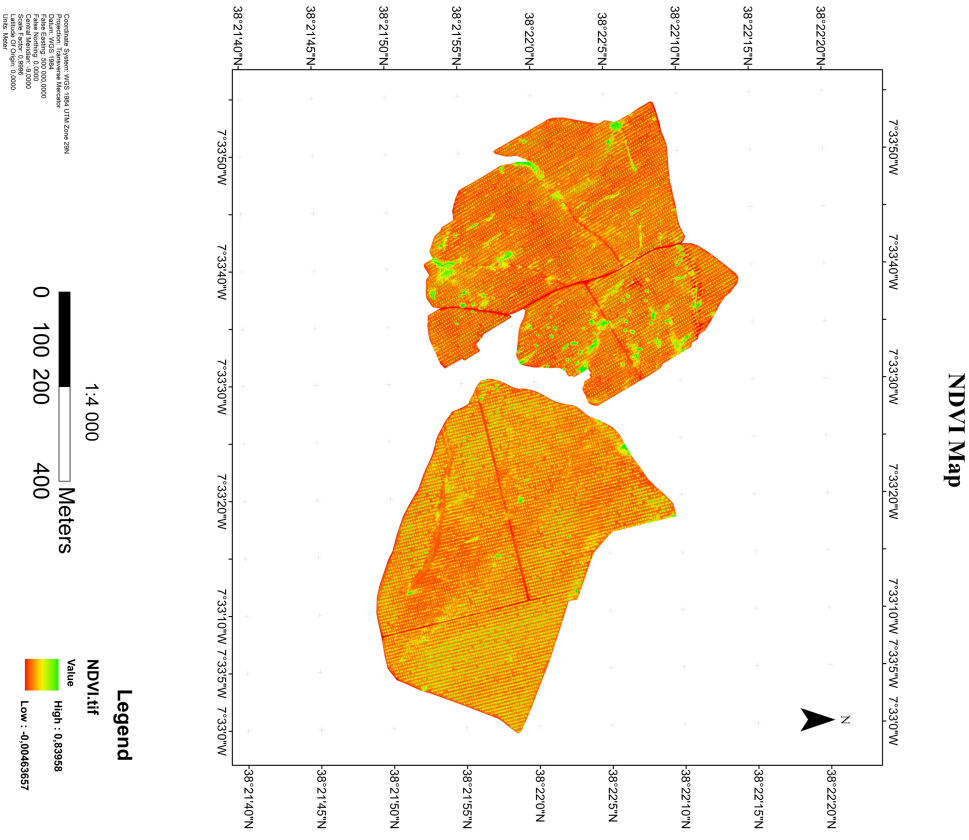

Figure 31. The original NDVI map for the olive grove.

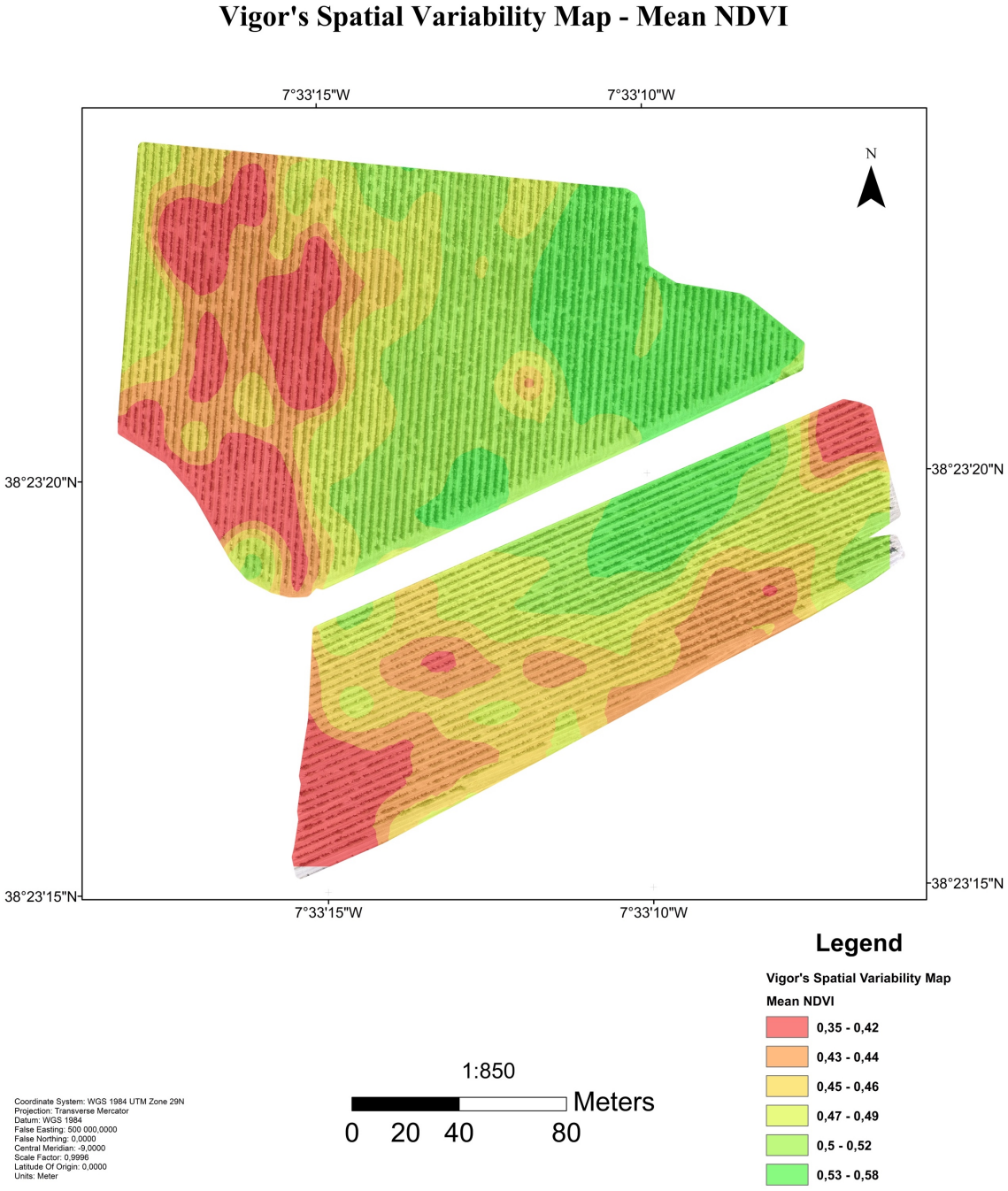

Figure 32. Final Vigor's Variability Map for the vineyard.

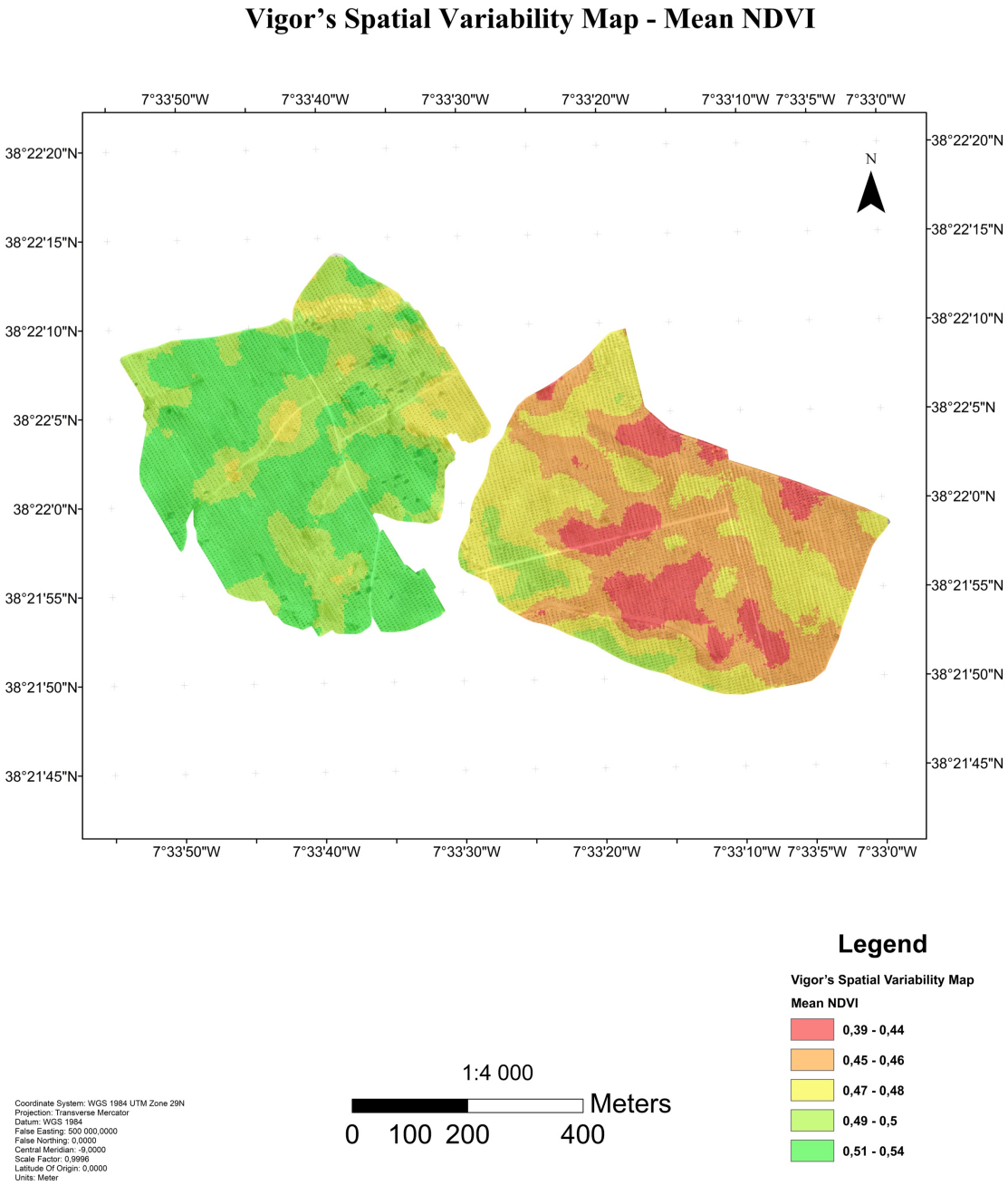

Figure 33. Final Vigor's Variability Map for the olive grove.

5 DISCUSSION

The high resolution Vegetation Index Maps for agricultures with low density crops result in raster's surfaces difficult to interpret, making it challenging to identify the vigor's spatial patterns present. In other cases, low resolution images represent an average between the vegetation canopy and the soil

around it, thus not representing the intra-canopy spatial variability. However, in order to fully take advantage of this resolution gap UAS creates, it is necessary to increase the knowledge of the growing number of intervening variables that cause this variability. For this same purpose other types of sensors and Vegetation Indexes can be used as input for the canopies' polygon data, depending on the objectives or problems, taking advantage of the classification and interpolation methodology proposed here. It is important to notice that the need for geo-referencing the different bands between them is caused only from using different UAS, one for the RGB and other for the Multispectral bands, this can be avoided if an integrated solution is used. In the Principal Components Analysis is possible to notice that variables that were calculated using the same sensor had higher correlations between them since each has different wavelengths specifications. The use a UAS capable of capturing multiple bands in the same flight, including the RGB and the Multispectral bands would simplify the methodology proposed and possibly give better results since the geo-referencing stage and the resolution differences would be redundant. Due to the intertwined physiognomy of the vineyard, in the classification phase more than one point was placed in each polygon, since each polygon was representing a vector of vines. The same was tested but using the Max Value present in each polygon and also the original NDVI raster to extract the raster cell value directly to each point rather than calculating a mean of the NDVI values and the results showed to be comparable to the method here proposed. This second test was done with the objective of confirming if, in the vine classification, the mean NDVI per polygon calculation was diluting the spatial variability in the data, however the same spatial patterns were identified. It would be interesting to analyse the temporal variability with this method, allowing the visualization of the phenomena distribution in a plot level. This would also help studying plant maturity transitions, yield estimation, diseases or results from interventions made to the soil or crops, if correlation between the spatial variability vigor's maps and other factors known to affect the culture are found. For that purpose, planning the collection phase requires similar flight characteristics in terms of outputs' resolution, sensors used in each flight,

calibrations and image overlap in order for the methodology to be used in a repetitive temporal analysis.

6 CONCLUSIONS

In this dissertation, from remote sensing technologies, spatial analysis tools and Unmanned Aerial Systems a canopy pixel classification was developed in order to map the pure vigor of the canopies. The NDVI values were extracted from these canopies, enabling the study of the vigor in the vineyard's and olive grove's canopies ignoring the soil NDVI values. In both cases, clustered patterns of the mean NDVI were found, showing areas where canopy mean NDVI values are higher, reaching values around 0,6 and lower with values around 0,35. Data neither exhibited an overall anisotropic pattern, global trend nor proportional effect. While in the olive grove, even with the presence of Oak trees in the study area, tree boundaries were segmented and single olive trees could be identified (14000 olive trees counted), in vineyard was not possible to discriminate single Vines and their borders, resulting from the vegetation dense physiognomy. From the Vigor's Spatial Variability maps produced was possible to identify different vigor patterns, otherwise hidden with the noise caused by the soil. These predicted surface maps reveal useful information and can be used as a spatial variability visualization tool to support decision making, identifying critical areas to be managed separately, study plant maturity transitions, diseases, analyse results from interventions to the soil or crops or estimating yearly yields. These maps can also be used in VRT applications for prescription mapping or used to segment irrigation areas, optimizing productivity, sustainability and costs.

BIBLIOGRAPHIC REFERENCES

BALUJA, J., DIAGO, M. P., BALDA, P., ZORER, R., MEGGIO, F., MORALES, F., and TARDAGUILA, J., 2012, Assessment of vineyard water status variability by thermal and multispectral imagery using an unmanned aerial vehicle (UAV). *Irrigation Science*, 30, 6, 511-522.

Esporão, 2017, [Caracteristicas da Herdade do Esporão] (Évora).

GITELSON, A., KAUFMAN, Y., and MERZLYAK, M., 1996, Use of a green channel in remote sensing of global vegetation from EOS-MODIS, *Remote Sensing* of Environment, 58, 3, 289-298.

MATESE, A., TOSCANO, P., GENNARO, S. D., GENESIO, L., VACCARI, F., PRIMICERIO, J. and GIOLI, B., 2015. Intercomparison of UAV, Aircraft and Satellite Remote Sensing Platforms for Precision Viticulture. *Remote Sensing*, 7, 3, 2971-2990.

ORTEGA, R. and ESSER, A., 2002. Viticultura de Precisión: Fundamentos, aplicaciones y oportunidades en Chile. Pontificia Universidad Católica de Chile. 1-10.

PINTO, M., 2015. Viticultura de Precisão: Avaliação da variabilidade espacial da produtividade e qualidade na casta Touriga Nacional no Alentejo. Doctoral dissertation, ISA/UL, Lisboa.

PROFFITT, B., BRAMLEY R., LAMB, D. and WINTER, E., 2006. Precision Viticulture : A New Era in Vineyard Management and Wine Production. Ashford: Winetitles.

RIBÉREAU-GAYON, P., DUBOURDIEU, D., DONÈCHE, B. and LONVAUD, A., 2006. Handbook of Enology, Volume 1: The Microbiology of Wine and Vinifications. (2ª ed.) (John Wiley & Sons)

ROUSE, J., HAAS, R., SCHELL, J., DEERING, D. and HARLAN, J., 1974. Monitoring the vernal advancement and retrogradation (Greenwave effect) of natural vegetation. *NASA/GSFCT Type III Final Report*, Greenbelt, MD, USA.

SALAMÍ, E., BARRADO, C., and PASTOR, E., 2014. UAV Flight Experiments Applied to the Remote Sensing of Vegetated Areas. *Remote Sensing*, 6(11), 11051-11081.

TOKEKAR, P., HOOK, J., MULLA, D. and ISLER, V., 2013. Sensor planning for a symbiotic UAV and UGV system for precision agriculture. *In Proceedings of 2013 IEEE/RSJ International Conference on Intelligent Robots and Systems (IROS),* pp. 5321–5326.

XIANG, H. and TIAN, L., 2011. Development of a low-cost agricultural remote sensing system based on an autonomous unmanned aerial vehicle (UAV). *Biosyst. Eng*., 108, 174–190.

ZARCO-TEJADA, P., GONZÁLEZ-DUGO, V. and BERNI, J., 2012. Fluorescence, temperature and narrow-band indices acquired from a UAV platform for water stress detection using a micro-hyperspectral imager and a thermal camera. Remote Sensing of Environment, 117, 322–337.

Masters Program in Geospatial Technologies

PRECISION AGRICULTURE USING UNMANNED AERIAL SYSTEMS

Mapping Vigor's Spatial Variability on Low Density Agricultures using a Canopy Pixel Classification and Interpolation Model

Pedro Pais Penedos

Dissertation submitted in partial fulfilment of the requirements for the Degree of *Master of Science in Geospatial Technologies*

NOVA IMS Information Management School
Universitat Jaume I
Westfälische Wilhelms-Universität Münster

Masters Program in **Geospatial Technologies**

Supported by:
Education and Culture
ERASMUS MUNDUS